© 2016. Published by The Company of Biologists Ltd | Journal of Cell Science (2016) 129, 2660-2672 doi:10.1242/jcs.181768

RESEARCH ARTICLE

Kinectin-dependent ER transport supports the focal complex maturation required for chemotaxis in shallow gradients

Inn Chuan Ng[1,2], Pornteera Pawijit[1,2], Lee Ying Teo[2], Huipeng Li[3], Shu Ying Lee[4] and Hanry Yu[1,2,3,4,5,6,7,8,*]

ABSTRACT

Chemotaxis in shallow gradients of chemoattractants is accomplished by preferential maintenance of protrusions oriented towards the chemoattractant; however, the mechanism of preferential maintenance is not known. Here, we test the hypothesis that kinectin-dependent endoplasmic reticulum (ER) transport supports focal complex maturation to preferentially maintain correctly oriented protrusions. We knocked down kinectin expression in MDA-MB-231 cells using small interfering RNA and observed that kinectin contributes to the directional bias, but not the speed, of cell migration. Kymograph analysis revealed that the extension of protrusions oriented towards the chemoattractant was not affected by kinectin knockdown, but that their maintenance was. Immunofluorescence staining and live-cell imaging demonstrated that kinectin transports ER preferentially to protrusions oriented towards the chemoattractant. ER then promotes the maturation of focal complexes into focal adhesions to maintain these protrusions for chemotaxis. Our results show that kinectin-dependent ER distribution can be localized by chemoattractants and provide a mechanism for biased protrusion choices during chemotaxis in shallow gradients of chemoattractants.

KEY WORDS: Kinectin, Endoplasmic reticulum, Focal complex maturation, Chemotaxis

INTRODUCTION

Cell migration, the movement of cells from one location to another, is involved in physiological and disease processes such as embryogenesis, regeneration, the immune response and tumor metastasis (Devreotes and Janetopoulos, 2003; Swaney et al., 2010). It is orchestrated by coordinated steps of protrusion extension and maintenance, translocation of the cell body and retraction of the rear (Lauffenburger and Horwitz, 1996; Ridley et al., 2003). Protrusion extension refers to the forward movement of plasma membrane by local actin polymerization (Pollard and Borisy, 2003). Protrusion maintenance, by contrast, is achieved by adherence of membrane extensions to the substratum through the interaction of integrins with the extracellular matrix at focal adhesions (Beningo et al., 2001). Strong anchoring of leading protrusions to the substratum through focal adhesions is essential to support myosin-II-mediated contraction of actin filaments for translocation of the cell body and retraction of the rear (Gupton and Waterman-Storer, 2006). Weak anchoring results in slippage and collapse of leading protrusions, preventing the cell from generating enough contraction force to pull itself forward.

Cell migration is intrinsically driven and can be externally directed by extracellular cues such as chemoattractants (Petrie et al., 2009). Directional movement of cells in response to chemoattractants is called chemotaxis. Cell behavior during chemotaxis is dependent on the gradient of chemoattractants (Arrieumerlou and Meyer, 2005). In shallow gradients, cells migrate towards the chemoattractant in a biased random manner. Cells produce random protrusions, and protrusions oriented towards the chemoattractant are maintained whereas incorrectly oriented protrusions are retracted. The mechanism in which one protrusion is maintained while the other retracts is not well understood (Andrew and Insall, 2007). In steep gradients, cells migrate persistently towards the chemoattractant. New protrusions are induced in the direction of the chemoattractant.

Various studies have shown the involvement of endoplasmic reticulum (ER) transport in adhesion dynamics during cell migration (Burdisso et al., 2013; Yang et al., 2009; Zhang et al., 2010). ER is transported along microtubules (MTs) to the cell periphery by the tip-attachment complex (TAC) and sliding mechanisms (Friedman et al., 2010; Terasaki et al., 1986; Waterman-Storer and Salmon, 1998). Disruption of either ER transport mechanism has been shown to reduce cell migration (Yang et al., 2009; Zhang et al., 2010). The sliding mechanism is mediated by the microtubule (MT) motor protein kinesin-1. The main interaction partner of kinesin-1 on the ER is kinectin, an integral ER membrane protein. Full-length human kinectin is 1357 amino acids; it interacts with kinesin-1 from amino acid residues 1188–1288 (Kumar et al., 1995; Ong et al., 2000; Toyoshima et al., 1992; Wozniak et al., 2009). Disruption of the kinectin–kinesin-1 interaction through knockdown of kinectin or expression of the kinesin-1-binding domain of kinectin (KNT^{+}) results in ER retraction from the cell leading edge. Loss of ER contact with adhesions at the leading edge leads to reduced adhesion maturation and growth (Santama et al., 2004; Zhang et al., 2010). Reduced cell migration after disruption of the kinectin–kinesin-1 interaction might be due to changes in ER-dependent adhesion dynamics at the leading edge.

In this paper, we test the hypothesis that kinectin mediates ER transport preferentially to correctly oriented protrusions to promote focal complex maturation and thus maintain these protrusions during chemotaxis in shallow gradients. We knocked down the expression of kinectin and quantified its impact on various aspects of leading edge dynamics during chemotaxis in shallow gradients.

[1]NUS Graduate School of Integrative Sciences and Engineering, National University of Singapore, Singapore 117456, Singapore. [2]Department of Physiology, Yong Loo Lin School of Medicine, National University of Singapore, Singapore 117597, Singapore. [3]Singapore-MIT Alliance, E4-04-10, 4 Engineering Drive 3, Singapore 117576, Singapore. [4]Confocal Microscopy Unit, Yong Loo Lin School of Medicine, National University of Singapore, Singapore 117549, Singapore. [5]Mechanobiology Institute, National University of Singapore, Singapore 117411, Singapore. [6]Institute of Bioengineering and Nanotechnology, A*STAR, Singapore 138669, Singapore. [7]Singapore-MIT Alliance for Research and Technology, 1 CREATE Way, #10-01 CREATE Tower, Singapore 138602, Singapore. [8]Department of Biological Engineering, Massachusetts Institute of Technology, Cambridge, MA 02139, USA.

*Author for correspondence (phsyuh@nus.edu.sg)

H.Y., 0000-0002-0339-3685

Received 9 October 2015; Accepted 19 May 2016

Journal of Cell Science (2016) 129, 2660-2672 doi:10.1242/jcs.181768

We demonstrate that kinectin knockdown affects the directional bias but not the speed of cell migration. It does so by mediating ER transport preferentially to the periphery of protrusion most correctly oriented towards the chemoattractant. ER accumulation mediates protrusion maintenance by promoting the maturation of transient focal complexes into focal adhesions, providing strong adhesion to the substratum. Reduced focal adhesion formation is a probable cause for the loss of preferential maintenance of protrusions after kinectin knockdown.

RESULTS

Kinectin contributes to the directional bias but not the speed of cell migration

We have previously shown that the migration of HeLa cells in Transwell chemotaxis and wound healing assays is reduced by kinectin knockdown (Zhang et al., 2010). Here, we chose the highly migratory MDA-MB-231 cell line as a model to study the role of kinectin in cell migration. The expression of kinectin in MDA-MB-231 cells was knocked down using small interfering RNA (siRNA). Kinectin siRNA was designed to target nucleotides 720–744 of human kinectin mRNA (GenBank accession number ZZ22551), whereas the negative control siRNA was a scrambled sequence of kinectin siRNA which lacks significant similarity to human genes. For validation of kinectin knockdown, we used a polyclonal antibody against the C-terminus of human kinectin. Western blot and immunofluorescence staining results confirmed that the expression of kinectin in MDA-MB-231 cells was successfully knocked down after kinectin siRNA treatment (Fig. 1A).

We performed Transwell chemotaxis and wound healing assays on MDA-MB-231 cells to determine whether kinectin knockdown similarly reduced the migration of MDA-MB-231 cells as it does in HeLa cells. In a Transwell chemotaxis assay, migration of kinectin-knockdown cells towards fetal bovine serum (FBS) was reduced by 60% (Fig. 1Ba). In a wound healing assay, migration of kinectin-knockdown cells was reduced to 42% that of control cells (Fig. 1Bb). These results confirm that kinectin also contributes to the migration of MDA-MB-231 cells.

Transwell chemotaxis and wound healing assays measure the intrinsic ability of cells to migrate and be directed by external cues, which are chemoattractant and wounding, respectively. Intrinsic migration can be characterized by the velocity and persistence of migration, whereas directed migration can be additionally characterized by directional bias (Harms et al., 2005; Pankov et al., 2005; Petrie et al., 2009). To determine whether kinectin knockdown affects intrinsic migration, a random migration assay was performed. Live imaging of MDA-MB-231 cells in growth medium was performed at 10-min intervals over a period of 6 h (Fig. 1C). We observed that both control and kinectin-knockdown cells adopted the mesenchymal migration mode; cells migrated by forming protrusions that ranged from circumferential to narrow lamella. However, kinectin-knockdown cells had more pronounced membrane ruffles at leading edges during migration (Movies 1 and 2). Migration tracks of individual cells were also acquired by recording the coordinates of the cell body in each frame of a time-lapse image and drawing straight lines to connect subsequent coordinates. Velocity and persistence, which respectively represent the speed and efficiency of cell migration, were calculated from these sets of coordinates. Control and kinectin-knockdown cells had similar migration tracks (Fig. 1D). Velocity and persistence of migration were not significantly affected by knockdown of kinectin (Fig. 1E). These results show that kinectin is dispensable for intrinsic migration of MDA-MB-231 cells.

Given that the velocity and persistence of migration were not affected by knockdown of kinectin, the directional bias of migration might be affected instead. To characterize the directional bias of migration, we observed chemotaxis of MDA-MB-231 cells towards FBS in a Dunn chamber. Live imaging was performed at 10-min intervals over a period of 12 h, and cell migration tracks of 100 control and 63 kinectin-knockdown cells were analyzed. A Rayleigh test showed that the distribution of migration direction was biased for the control but not for the kinectin-knockdown cells (Fig. 2A). The chemotactic index and forward migration index in the y-direction (yFMI) further showed that the distribution of migration direction for control cells was biased towards the chemoattractant (Fig. 2B). Knockdown of kinectin impaired directional bias of migration towards the chemoattractant, causing the cells to migrate randomly. Meanwhile, control cells had biased random migration, a characteristic of chemotaxis in shallow gradients; the migration tracks of control cells were similar to randomly migrating kinectin-knockdown cells, but were biased towards the direction of the chemoattractant (Fig. 2C). We also noted that the velocity and persistence of chemotaxis were not affected by knockdown of kinectin (Fig. S1A). Our results indicate that kinectin contributes to directional bias of migration towards the chemoattractant during chemotaxis in shallow gradients.

Kinectin interacts with and performs its functions through kinesin-1 (Ong et al., 2000). Disruption of the kinectin–kinesin-1 interaction through the expression of KNT^+, a peptide with a sequence corresponding to the kinesin-1-binding domain of kinectin, has been reported to produce similar phenotypes to knockdown of kinectin (Zhang et al., 2010). Therefore, for validation, we compared chemotaxis results after the knockdown of kinectin to upon the expression of KNT^+. Cells were transfected with either GFP^+, an empty green fluorescent protein (GFP) vector, or GFP–KNT^+, a fusion construct of GFP and KNT^+. The cell migration tracks of 19 GFP^+ and 20 GFP–KNT^+ cells were analyzed. We found that chemotaxis results after the expression of KNT^+ were similar to those after knockdown of kinectin. Directional bias of migration towards the chemoattractant was impaired by the expression of KNT^+ (Fig. 2D–F) whereas velocity and persistence were unaffected (Fig. S1B). Taken together, our results indicate that kinectin contributes to chemotaxis in shallow gradients through its interaction with kinesin-1.

Kinectin mediates preferential maintenance of protrusions oriented towards the chemoattractant

To elucidate the process by which kinectin contributes to the directional bias of migration, the mode of cell migration during chemotaxis was characterized (Movies 3 and 4). Control cells were elongated and predominantly migrated by forming distinct lamellar protrusions (Fig. 3Aa). In contrast, kinectin-knockdown cells were mostly rounded and had pronounced membrane ruffles (Fig. 3Ab). After knockdown of kinectin, cells still formed lamellar protrusions in the direction of the chemoattractant (Fig. 3B), but did not migrate in that direction (Fig. 2A,B). Lamellar protrusions formed by kinectin-knockdown cells were not maintained and retracted back towards the cell body. This result suggests that kinectin-knockdown cells can still sense and respond to the chemoattractant, but have impaired lamellar protrusion dynamics compared to control cells.

Analysis of cell morphology showed that although the number of lamellar protrusions per cell was not significantly different; lamellar protrusion length of kinectin-knockdown cells was shortened by 45% when compared to control cells (Fig. 3C). Lamellar protrusion dynamics is mediated by extension and maintenance processes,

Journal of Cell Science (2016) 129, 2660-2672 doi:10.1242/jcs.181768

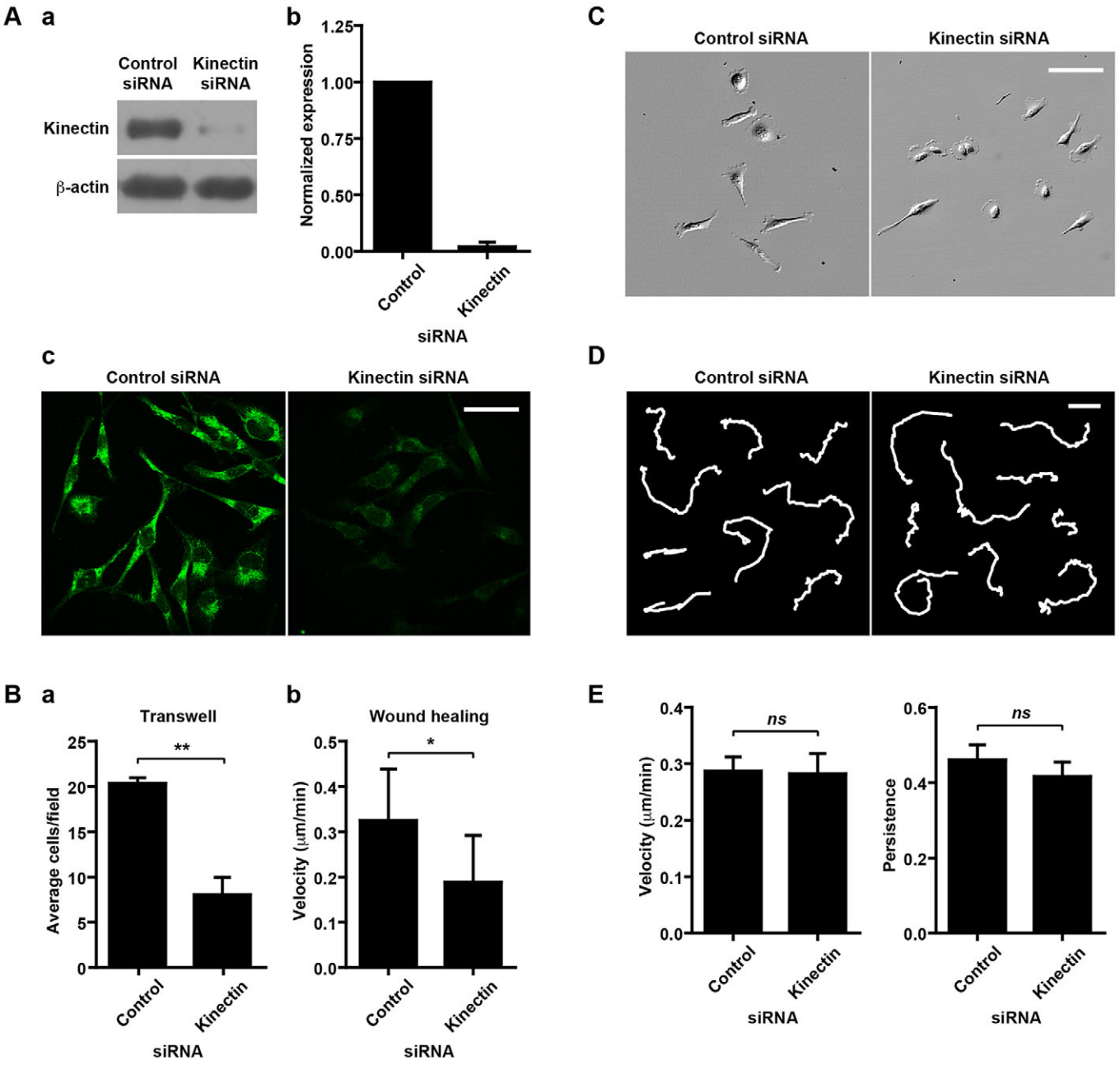

Fig. 1. Knockdown of kinectin reduces cell migration without affecting the velocity and persistence of migration. (A) MDA-MB-231 cells were treated with 40 nM control or kinectin siRNA. (a) Western blotting showed that kinectin expression was reduced after 96 h. (b) Average band intensity from three different knockdown experiments indicated that the percentage of knockdown was 96.0±3.6%. (c) Immunofluorescence staining demonstrating the expression and distribution of kinectin after siRNA treatment. Scale bar: 50 µm. (B) Knockdown of kinectin reduced cell migration during Transwell chemotaxis (control siRNA, 20.37±0.60 cells/field; kinectin siRNA, 8.08±1.92 cells/field) and wound healing assays (control siRNA, 0.33±0.11 µm/min; kinectin siRNA, 0.19±0.10 µm/min). **P*<0.05; ***P*<0.01 (paired two-tailed Student's *t*-test). (C) Morphologies of siRNA-treated MDA-MB-231 cells during random migration in a uniform chemoattractant concentration. Cells were seeded on glass coated with 10 µg/ml fibronectin and allowed to migrate in growth medium. Scale bar: 100 µm. (D) Representative migration tracks of siRNA-treated cells over a 12-h period. Scale bar: 50 µm. (E) Random migration was unaffected by kinectin knockdown. Analysis of migration tracks showed that the velocity (control siRNA, 0.287±0.025 µm/min; kinectin siRNA, 0.283±0.035 µm/min; *P*=0.92) and persistence of cell migration (control siRNA, 0.46±0.04; kinectin siRNA, 0.42±0.04; *P*=0.45) were not significantly affected. *ns*, not significant (unpaired two-tailed Student's *t*-test). Error bars in Ab, B and E represent the s.e.m. from at least three independent experiments.

which, respectively, involve forward movement of lamellipodia mediated by actin polymerization and cell adhesion to the substratum (Lauffenburger and Horwitz, 1996; Ridley et al., 2003). To assess the involvement of kinectin in protrusion maintenance, the persistence of lamellar protrusions during chemotaxis was tracked over a period of 8 h; protrusions oriented towards and away from the chemoattractant were analyzed separately because protrusion dynamics might be spatially regulated by the chemoattractant gradient. We observed that the mean persistence of protrusions oriented towards the chemoattractant in kinectin-knockdown cells was 55% lower compared to in control cells (Fig. 3D). However, no difference for protrusions oriented away from the chemoattractant was observed. Taken together, our results indicate that kinectin

Journal of Cell Science (2016) 129, 2660-2672 doi:10.1242/jcs.181768

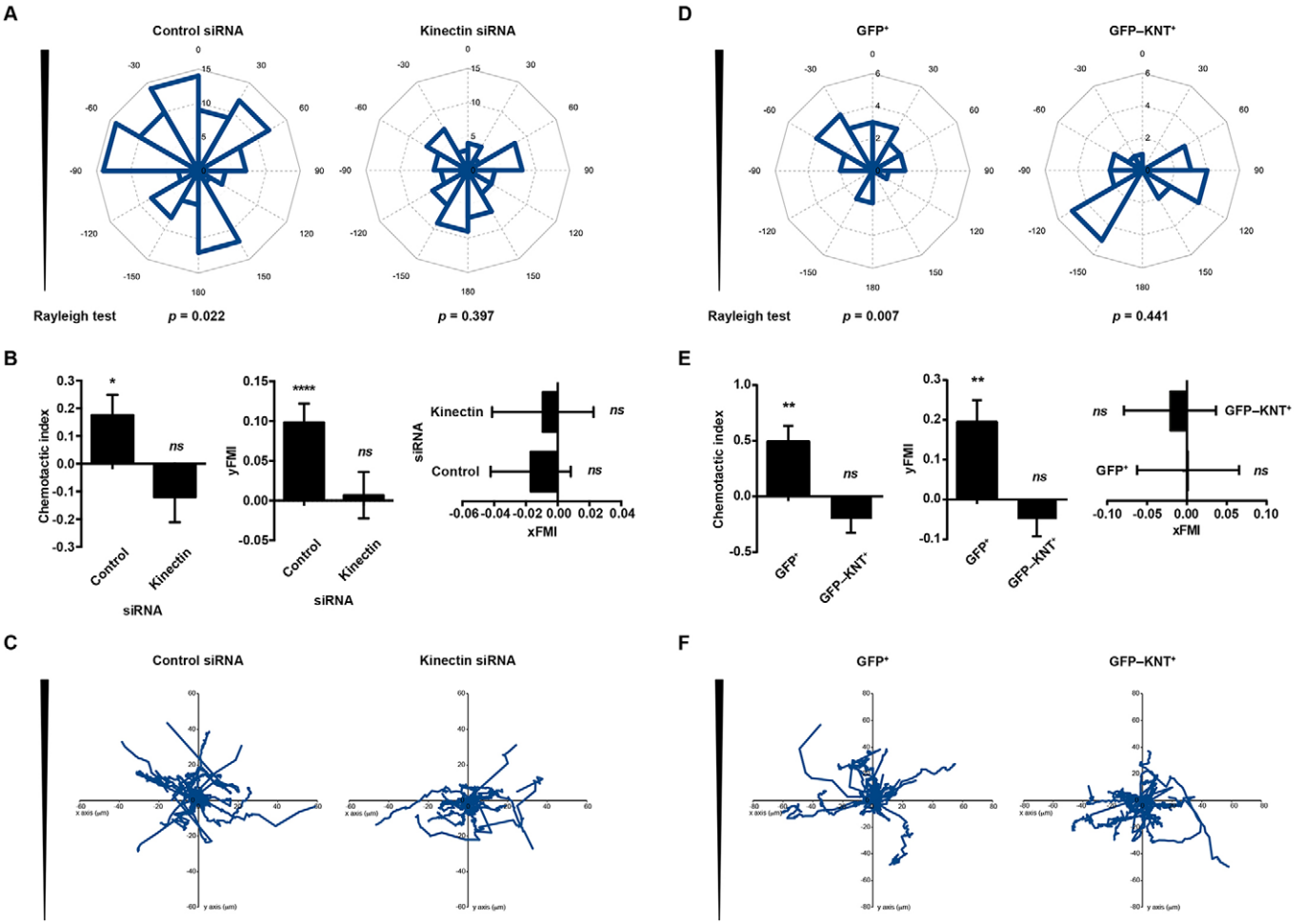

Fig. 2. Kinectin contributes to directional bias of cell migration during chemotaxis in shallow gradients through interaction with kinesin-1. (A) Rose plots and Rayleigh test showing that the migration of control but not kinectin-knockdown cells is directionally biased. Direction of the chemoattractant gradient is towards the top. Chemotaxis of siRNA-treated MDA-MB-231 cells towards FBS was imaged in a Dunn chamber at 10-min intervals over a 12-h period. A total of 100 control and 63 kinectin-knockdown cells were quantified. (B) Kinectin-mediated directional bias of cell migration towards the chemoattractant. Chemotactic index (control siRNA, 0.176±0.074, P=0.019; kinectin siRNA, −0.120±0.091, P=0.190) and forward migration index in the y-direction (yFMI; control siRNA, 0.098±0.024, P=0.00007; kinectin siRNA, −0.120±0.091, P=0.190) were significant for control but not kinectin-knockdown cells. Forward migration index in the x-direction (xFMI) was not significant for both control and kinectin-knockdown cells. Error bars represent s.e.m. *P<0.05; ****P<0.0001; *ns*, not significant for the result compared to a hypothetical value of 0.00 (one-sample t test). (C) Representative migration tracks of siRNA-treated cells undergoing chemotaxis. (D) Rose plots and Rayleigh test showing that the migration of GFP$^+$ but not GFP–KNT$^+$ cells was directionally biased. Direction of the chemoattractant gradient is towards the top. GFP$^+$ is an empty GFP vector whereas GFP–KNT$^+$ is a fusion construct of GFP to the kinesin-1-binding domain of kinectin (KNT$^+$). Chemotaxis of transfected MDA-MB-231 cells towards FBS was imaged in a Dunn chamber at 10-min intervals over 12 h. A total of 19 cells expressing GFP$^+$ and 20 cells expressing GFP–KNT$^+$ were analyzed. (E) Directional bias towards the chemoattractant was mediated by kinectin–kinesin-1 interaction. Chemotactic index (GFP$^+$, 0.496±0.139, P=0.002; GFP–KNT$^+$, −0.203±0.124, P=0.119) and yFMI (GFP$^+$, 0.195±0.054, P=0.002; GFP–KNT$^+$, −0.049±0.043, P=0.271) were significant for GFP$^+$ but not GFP–KNT$^+$ cells. xFMI was not significant for both GFP$^+$ and GFP–KNT$^+$ cells. Error bars represent s.e.m.; **P<0.01; *ns*, not significant for the result compared to a hypothetical value of 0.00 (one-sample t-test). (F) Migration tracks of transfected cells undergoing chemotaxis.

mediates preferential maintenance of protrusions oriented towards the chemoattractant.

To describe the contribution of kinectin to lamellar protrusion extension, we recorded the lamellipodia movement of control and kinectin-knockdown cells. Kymographs of lamellipodia in protrusions oriented towards the chemoattractant of control cells formed distinctive peaks and troughs, whereas those in protrusions oriented away were less prominent (Fig. 3E). Lamellipodia formed in both directions of kinectin-knockdown cells were not prominent, and were comparable to those oriented away from the chemoattractant in control cells. The extension and retraction velocities of lamellipodia, parameters used in quantifying lamellipodia formation, in protrusions oriented towards and away from the chemoattractant were not significantly affected by knockdown of kinectin (Fig. 3F). However, knockdown of kinectin slightly, but significantly, increased the frequency and reduced the amplitude of lamellipodia in protrusions oriented towards, but not away from, the chemoattractant (Fig. 3G). These results suggest that kinectin is not involved in lamellipodia formation, as lamellipodia extension and retraction velocities were comparable to those in control cells, but might indirectly contribute to maintenance of lamellipodia in protrusions oriented towards the chemoattractant, as the amplitude and frequency of lamellipodia were affected.

Kinectin mediates bias in ER distribution to protrusions oriented towards the chemoattractant

We have previously shown in HeLa cells that kinectin mediates ER transport to leading edges to promote focal adhesion growth (Zhang

Journal of Cell Science (2016) 129, 2660-2672 doi:10.1242/jcs.181768

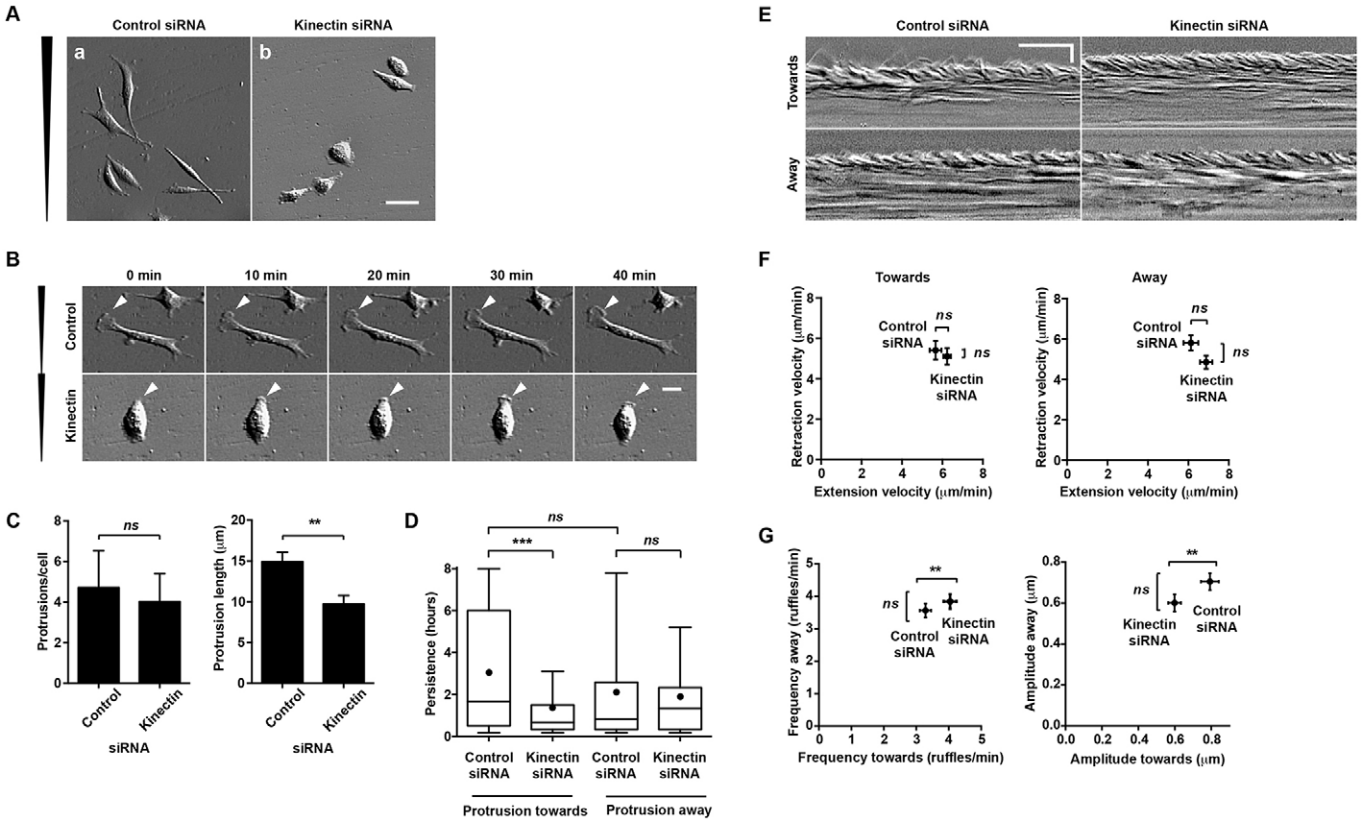

Fig. 3. Knockdown of kinectin affects maintenance but not extension of cell protrusions. (A) During chemotaxis in a Dunn chamber, control cells were elongated and formed distinct protrusions whereas kinectin-knockdown cells were rounded. The direction of the chemoattractant gradient is towards the top. Scale bar: 50 µm. (B) Time-lapse images during chemotaxis showing that kinectin-knockdown cells failed to form stable protrusions towards the chemoattractant. Protrusions of kinectin-knockdown cells were prone to collapse. Arrowheads indicate protrusions oriented towards the chemoattractant. The direction of the chemoattractant gradient is towards the top. Scale bar: 20 µm. (C) Quantification of 39 control and 41 kinectin-knockdown cells revealed that kinectin knockdown did not affect total cell protrusions but reduced protrusion length (control siRNA, 14.9±1.2 µm; kinectin siRNA, 9.7±1.1 µm). Error bars represent s.e.m. $^{**}P<0.01$; *ns*, not significant (unpaired two-tailed Student's *t*-test). (D) Kinectin mediates preferential maintenance of protrusions oriented towards the chemoattractant. A box plot shows that kinectin knockdown reduced the persistence of protrusions oriented towards (control siRNA, $n=96$, 3.01±0.31 h; kinectin siRNA, $n=75$, 1.37±0.22 h; mean±s.e.m.; $P=0.0002$) but not away from the chemoattractant (control siRNA, $n=81$, 2.10±0.29 h; kinectin siRNA, $n=81$, 1.91±0.24 h; mean±s.e.m.; $P=0.54$). Persistence over 8 h of chemotaxis was manually quantified. The box represents the 25–75th percentiles, and the median is indicated by the line; dots represent mean and whiskers the 10–90 percentiles. $^{***}P<0.001$; *ns*, not significant (one-way ANOVA with Tukey's multiple comparison test). (E) Representative kymographs show movement of lamellipodia in protrusions oriented towards and away from chemoattractant in control and kinectin-knockdown cells. Scale bars: vertical, 2 µm, horizontal, 60 s. (F) Kinectin did not contribute to lamellipodia formation during chemotaxis in shallow gradients. Analysis of kymographs determined that lamellipodia extension and retraction velocities in protrusions oriented towards (left graph) and away from the chemoattractant (right graph) were not affected. Error bars represent s.e.m. *ns*, not significant (unpaired two-tailed Student's *t*-test). (G) Kinectin contributed to the stability of lamellipodia in protrusions oriented towards the chemoattractant. Lamellipodia in protrusions oriented towards but not away from the chemoattractant of kinectin-knockdown cells had a slightly increased frequency (left graph) and reduced amplitude (right graph) compared to control cells. Error bars represent s.e.m. $^{**}P<0.01$; *ns*, not significant (unpaired two-tailed Student's *t*-test).

et al., 2010). Protrusion maintenance involves cell-adhesion to the substratum (Beningo et al., 2001); therefore, kinectin might contribute to preferential maintenance of lamellar protrusions through ER-dependent adhesion maturation and growth. First, we examined the correlation of ER distribution with protrusion maintenance. The ER was stained with cell-permeable dye ER Tracker Blue-White DPX and the dynamics of ER during chemotaxis in a Dunn chamber was recorded. Live-cell imaging showed that MDA-MB-231 cells formed multiple lamellar protrusions with different orientations. These protrusions could either be actively extending leading protrusions or be inactive. In a cell with protrusions at opposite ends (Movie 5), ER accumulated to the protrusion oriented towards the chemoattractant (Fig. 4Aa, filled arrowhead) and retracted from the protrusion oriented away from the chemoattractant (Fig. 4Aa, empty arrowhead). The protrusion with the ER became the new leading protrusion and extended forward, whereas the protrusion without ER slowly retracted backwards. ER distribution seems to be biased to protrusions oriented towards the chemoattractant. In a cell with bifurcated leading protrusions (Fig. 4Ab; Movie 6), ER accumulated to both protrusions (Fig. 4Ab, arrowheads), but was biased towards the protrusion that was more accurately oriented towards the chemoattractant (Fig. 4Ab, filled arrowhead). The protrusion with more ER was preferentially maintained and extended forward, whereas the protrusion with less ER (Fig. 4Ab, empty arrowhead) was left behind and later collapsed as the cell migrated in the opposing direction, suggesting that ER contributes to the maintenance of lamellar protrusions.

We further investigated whether kinectin mediates the bias in ER distribution to protrusions oriented towards the chemoattractant. Cells undergoing chemotaxis were immunolabeled for protein disulfide isomerase (PDI, also known as P4HB) and actin filaments to visualize the ER and cell morphology, respectively (Fig. 4B). In

Journal of Cell Science (2016) 129, 2660-2672 doi:10.1242/jcs.181768

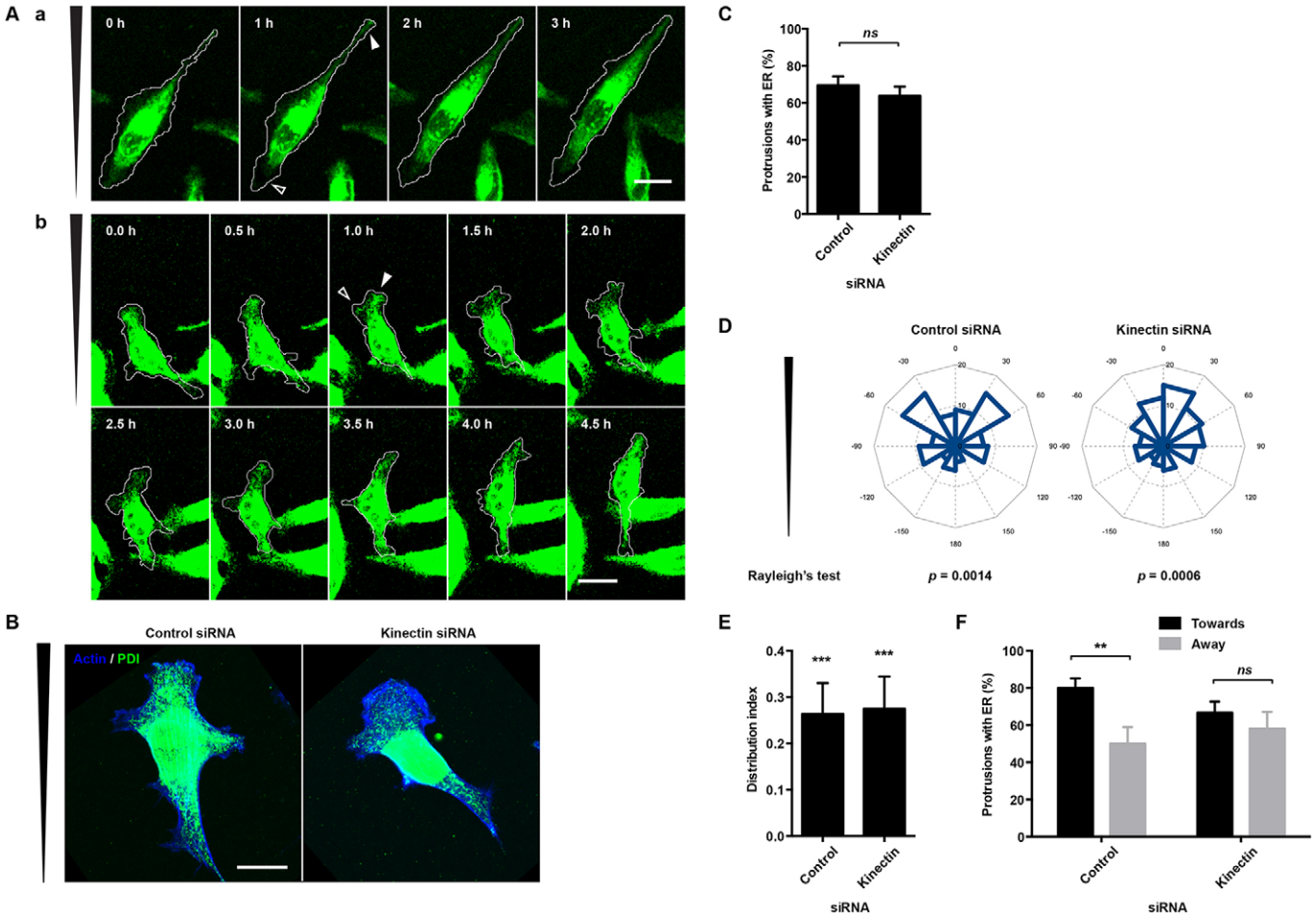

Fig. 4. Kinectin promotes ER accumulation to protrusions oriented towards the chemoattractant to preferentially maintain those protrusions. (A) Time-lapse images showing chemotaxis of MDA-MB-231 cells stained with the permeable dye ERTracker Blue (green) in a Dunn chamber. The direction of chemoattractant gradient is towards the top. In a cell with protrusions at opposing ends, ER accumulated to the protrusion oriented towards the chemoattractant and retracted from the protrusion oriented away from the chemoattractant (a). In a cell with two protrusions oriented towards the chemoattractant, ER preferentially accumulated to the protrusion which was more accurately oriented (b). ER accumulation led to maintenance of the protrusion. The protrusion which was less accurately oriented retracted after being left behind as the cell migrated forward. Filled arrowheads indicate protrusions with ER accumulation; open arrowheads indicate protrusions with ER retraction. Scale bars: 20 µm. (B) ER was retracted from the lamella and was reduced into globules and tubules in kinectin-knockdown MDA-MB-231 cells during chemotaxis in a Dunn chamber. Cells were stained for ER (anti-PDI; green) and actin (phalloidin; blue). The direction of chemoattractant gradient is towards the top. Scale bar: 20 µm. (C) The percentage of protrusions with observable ER in the lamella was not significantly different between control and kinectin-knockdown cells (control siRNA, 69.8±4.8%, *n*=92; kinectin siRNA, 63.8±5.0%, *n*=94; *P*=0.44). Error bars represent s.e.m. *ns*, not significant (Mann–Whitney test). (D) Rose plots and Rayleigh test showing that the orientation of protrusions in both control and kinectin-knockdown cells were directionally biased. The direction of chemoattractant gradient is towards the top. (E) The distribution of protrusion angles in control and kinectin-knockdown cells were biased towards the chemoattractant. ***$P<0.001$ for the result compared to a hypothetical value of 0.00 (one-sample *t* test). (F) ER in control (towards, *n*=60, 80.0%±5.2%; away, *n*=32, 50.0±9.0%; *P*=0.004) but not kinectin-knockdown cells (towards, *n*=63, 66.7±6.0%; away, 58.1±9.0%, *n*=31; *P*=0.495) were biased to protrusions oriented towards the chemoattractant. Error bars represent s.e.m. **$P<0.01$; *ns*, not significant (Mann–Whitney test).

control cells, the ER had a tubular reticular structure and was distributed almost to the lamella–lamellipodia interface. In kinectin-knockdown cells, the ER was retracted from the lamella, leaving residual ER in the form of tubules and globules, which is still consistent with the role of kinectin in ER structure and distribution (Santama et al., 2004). Although the intensity of ER staining in the lamella of kinectin-knockdown cells was severely reduced, ER distribution to the lamella–lamellipodia interface was not significantly affected; the presence of ER there could still be observed (Fig. 4C). Before determining the bias in ER distribution to leading protrusions during chemotaxis, we observed whether the protrusion distribution itself was biased. Our results show that the distribution of protrusions in control and kinectin-knockdown cells was biased towards the chemoattractant (Fig. 4D,E), indicating that both control and kinectin-knockdown cells were able to sense and partially respond to the chemoattractant. Given that the protrusion distribution was biased, we compared the percentage, rather than the total number, of protrusions that had ER present. In control cells, the percentage of protrusions with ER and oriented towards the chemoattractant was 1.6-fold higher than those oriented away from the chemoattractant (Fig. 4F), indicating that the ER distribution is biased to protrusions oriented towards the chemoattractant. In kinectin-knockdown cells, no significant difference was observed, indicating a loss of bias in ER distribution. We demonstrated that kinectin mediates bias in ER distribution to protrusions oriented towards the chemoattractant.

Journal of Cell Science (2016) 129, 2660-2672 doi:10.1242/jcs.181768

ER promotes adhesion growth and maturation for protrusion maintenance

To demonstrate the role of ER in adhesion growth, cells undergoing chemotaxis were also immunolabeled for vinculin, an adhesion marker (Fig. 5A). In control cells, adhesion plaques were found along the cell periphery and scattered within the lamella. The ER was in partial contact with adhesion plaques in the periphery and in full contact with those in the lamella. In kinectin-knockdown cells, adhesions plaques appeared to be two parallel layers along the cell periphery. The ER was in partial contact with the inner layer of adhesion plaques but not the outer layer. The area of adhesion plaques in protrusions was quantified and normalized to the perimeter length of protrusions. For both control and kinectin-knockdown cells, we observed that the normalized adhesion area was 1.3-fold higher in protrusions with ER than in those without ER (Fig. 5B), suggesting that ER contact encourages adhesion maturation and growth, in line with previous reports (Zhang et al., 2010).

To demonstrate that protrusions are maintained by ER-dependent cell adhesions, we compared protrusions of control and kinectin-knockdown cells during chemotaxis. A micropipette tip containing FBS was used to generate the chemoattractant gradient. The dynamics of ER and adhesions were visualized by coexpressing pDsRed2-ER with integrin-β3–GFP. The pDsRed2-ER vector expresses a fusion DsRed2 fluorescent protein that localizes to the ER, whereas integrin β3 is a component of early adhesions in the leading edge (Ballestrem et al., 2001; Zaidel-Bar et al., 2003) and, hence, integrin-β3–GFP labels these structures. The position of the cell periphery was determined from differential interference contrast (DIC) images. Integrin β3 localized to both focal complexes and focal adhesions of MDA-MB-231 cells (Fig. 6). Focal complexes ranged from small punctate dots of less than 1 µm in size to larger but diffused irregular-shaped plaques with weak fluorescence intensity. The diffused plaques, which were found only at the lamellipodia, might be newly formed focal complexes too small to be resolved by confocal microscope. Focal adhesions at the lamella had high fluorescence intensity and ranged from small rounded to large elongated plaques. In protrusions oriented towards the chemoattractant of control cells (Fig. 6, Fig. S2, Fig. S3; control siRNA), the ER maintained contact with focal complexes at the cell periphery as it advanced forward along with membrane extension. Focal complexes with ER contact matured into focal adhesions by increasing in size and intensity, while focal adhesions remained intact to stabilize the protrusions as they extended forward. In protrusions oriented towards the chemoattractant of kinectin-knockdown cells (Fig. 6, Fig. S2, Fig. S3; kinectin siRNA), the ER failed to keep up with membrane extension and often did not contact focal complexes at the cell periphery. The small, diffuse and dynamic focal complexes did not mature into focal adhesions and were insufficient to maintain cell protrusions. Occasionally, the cell periphery receded past these focal complexes, causing the focal complexes to disassemble, and resulting in the collapse of the whole protrusion. Dynamics of ER and adhesions in protrusions oriented away from the chemoattractant of control and kinectin-knockdown cells were similar (Fig. 7). ER did not contact focal complexes at the cell periphery and the membrane did not extend forward. This shows that ER contact promotes the maturation of focal complexes into focal adhesions to allow protrusion maintenance.

DISCUSSION

Anterograde ER transport by the sliding mechanism is mediated by kinesin-1. Kinesin-1 likely mediates ER sliding through kinectin, as disruption of kinectin–kinesin-1 interaction and knockdown of kinectin similarly reduced ER transport (Santama et al., 2004; Toyoshima et al., 1992; Wozniak et al., 2009). Perturbation of ER transport through knockdown of kinectin reduced the migration of HeLa cells by reducing focal adhesion growth (Zhang et al., 2010), but the exact process by which kinectin-dependent ER transport regulates cell migration remained to be studied. Here, we provide new insight into the contribution of kinectin-dependent ER transport to the dynamics of directed migration, and describe the process in which it regulates cell migration. Our central finding is that kinectin-dependent ER transport promotes preferential

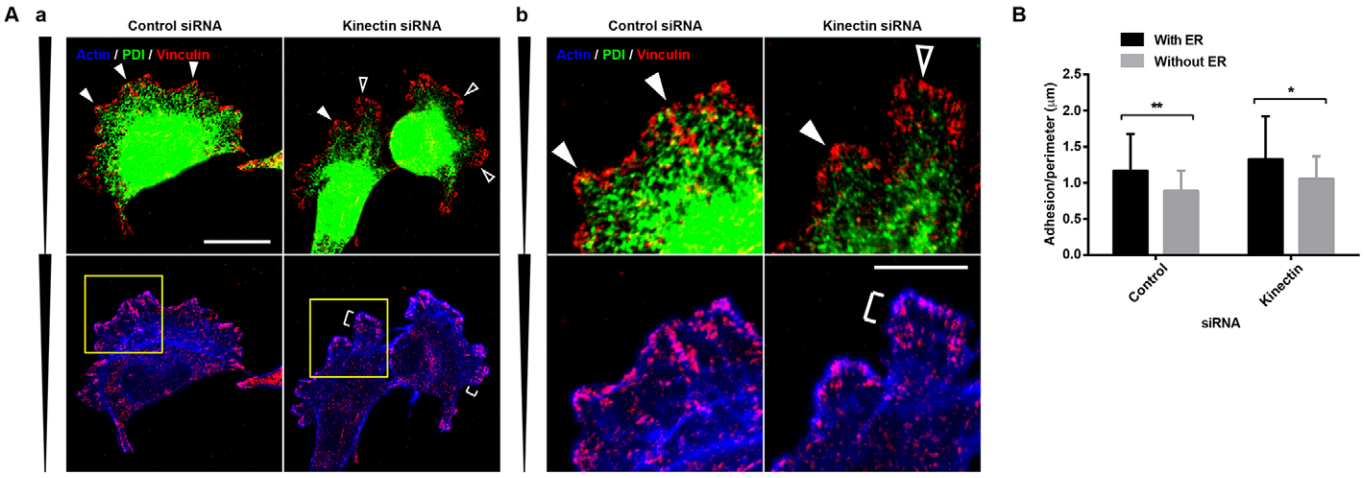

Fig. 5. ER promotes adhesion growth. (A) Morphology and distribution of adhesion plaques in control and kinectin-knockdown cells during chemotaxis in a Dunn chamber. Cells were stained for ER (PDI, green), adhesions (vinculin, red) and actin (phalloidin, blue). Filled arrowheads, adhesion plaques with ER contact; open arrowheads, adhesion plaques without ER contact; brackets, parallel layers of adhesion plaques. Panels in b are enlarged images of protrusions in a (yellow box). The direction of chemoattractant gradient is towards the top. Scale bars: 20 µm (a); 10 µm (b). (B) Comparison of normalized adhesion areas between leading protrusions with and without ER. In both control (with ER, n=64, 1.17±0.51 µm^2/µm; without ER, n=28, 0.89±0.28 µm^2/µm) and kinectin-knockdown cells (with ER, n=60, 1.33±0.59 µm^2/µm; without ER, n=34, 1.06±0.31 µm^2/µm), protrusions without ER had less adhesion. Error bars represent s.d. *P<0.05; **P<0.01 (unpaired two-tailed Student's t-test).

Journal of Cell Science (2016) 129, 2660-2672 doi:10.1242/jcs.181768

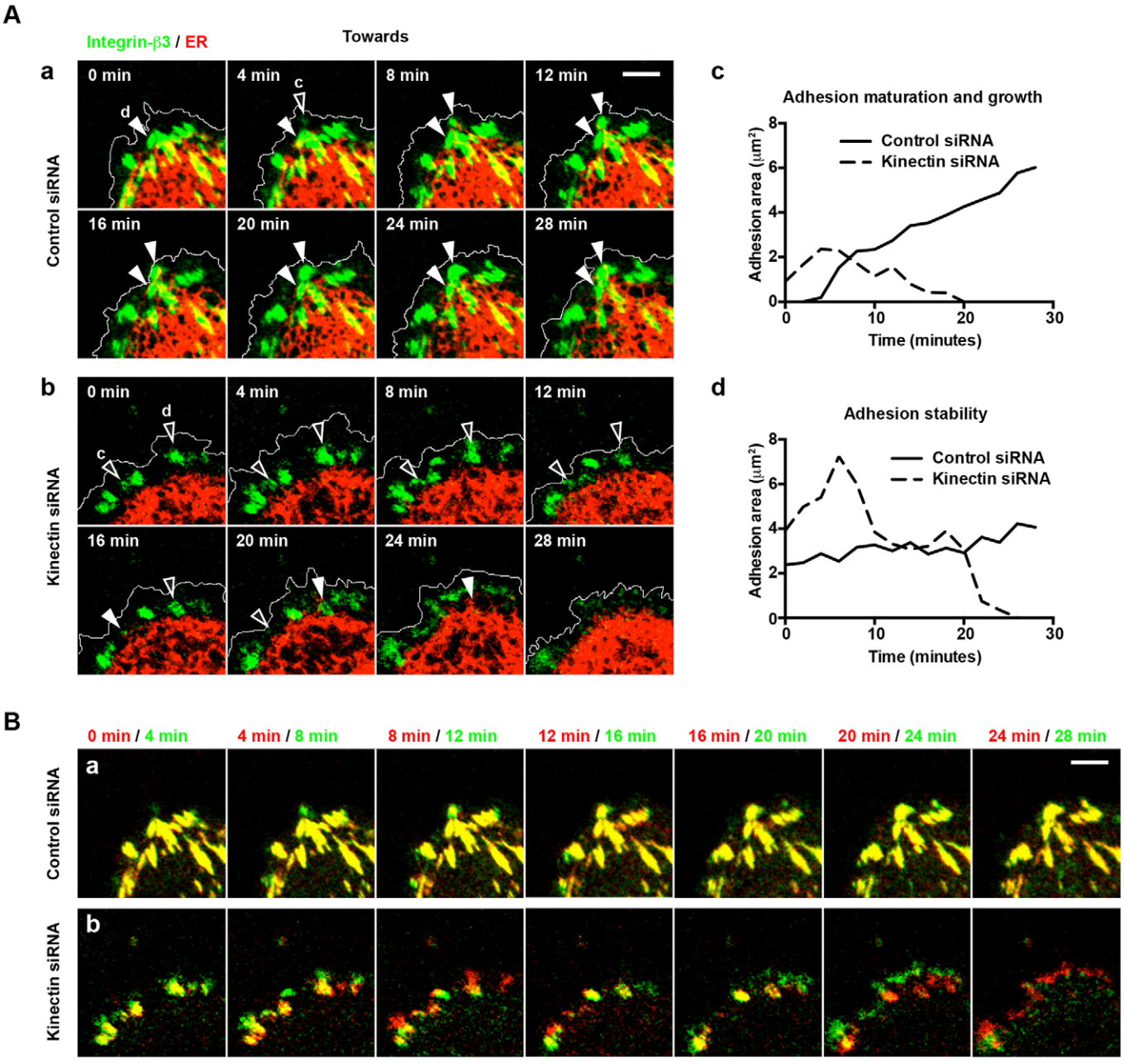

Fig. 6. Dynamics of ER and adhesions in protrusions oriented towards the chemoattractant. (A) Time-lapse images showing protrusions oriented towards the chemoattractant during chemotaxis. Cells were transfected with integrin-β3–GFP (green) and pDsRed2-ER (red). Cell edges (white lines) were determined from DIC images. A micropipette with FBS was placed at the top left, ~250 µm away. In protrusions oriented towards the chemoattractant of control cells (a), ER contact with focal complexes promoted the maturation of focal complexes to focal adhesions. Focal adhesions stabilized elongation of leading protrusion. In kinectin-knockdown cells (b), the ER did not contact focal complexes and focal complexes failed to mature into focal adhesions. Focal complexes were insufficient to stabilize the protrusion and disassembled as the protrusion collapses. Filled arrowheads, adhesions with ER contact; open arrowheads, adhesions without ER contact. Scale bar: 5 µm. (c,d) Quantification of the size of peripheral adhesions over time in a and b. The effects of focal complex maturation are represented as adhesion maturation and growth (c) and adhesion stability (d). (B) Timepoint overlays showing dynamics of integrin-β3–GFP adhesions in protrusions oriented towards the chemoattractant during chemotaxis. 'Current' and 'current+4 min' frames are colored red and green, respectively. Structures in green are new, structures in yellow are unchanged between frames and structures in red disassembled by the next frame. Scale bar: 5 µm.

maintenance of protrusions oriented towards the chemoattractant to direct cell migration during chemotaxis in shallow gradients of chemoattractants. By perturbing ER transport through knockdown of kinectin, we demonstrate that kinectin-dependent ER transport contributes to the directional bias, but not the velocity and persistence, of migration. Kinectin transports ER preferentially to protrusions oriented towards the chemoattractant. ER then promotes the maturation of focal complexes to focal adhesions to maintain these protrusions for directioned migration.

Cells are able to detect a front-to-back difference in chemoattractant concentration of as low as 2% (Devreontes and Zigmond, 1988). Effects attributed to chemotaxis in shallow gradients of chemoattractants have reportedly been observed in 2–6% front-to-back differences in chemoattractant concentration

Journal of Cell Science (2016) 129, 2660-2672 doi:10.1242/jcs.181768

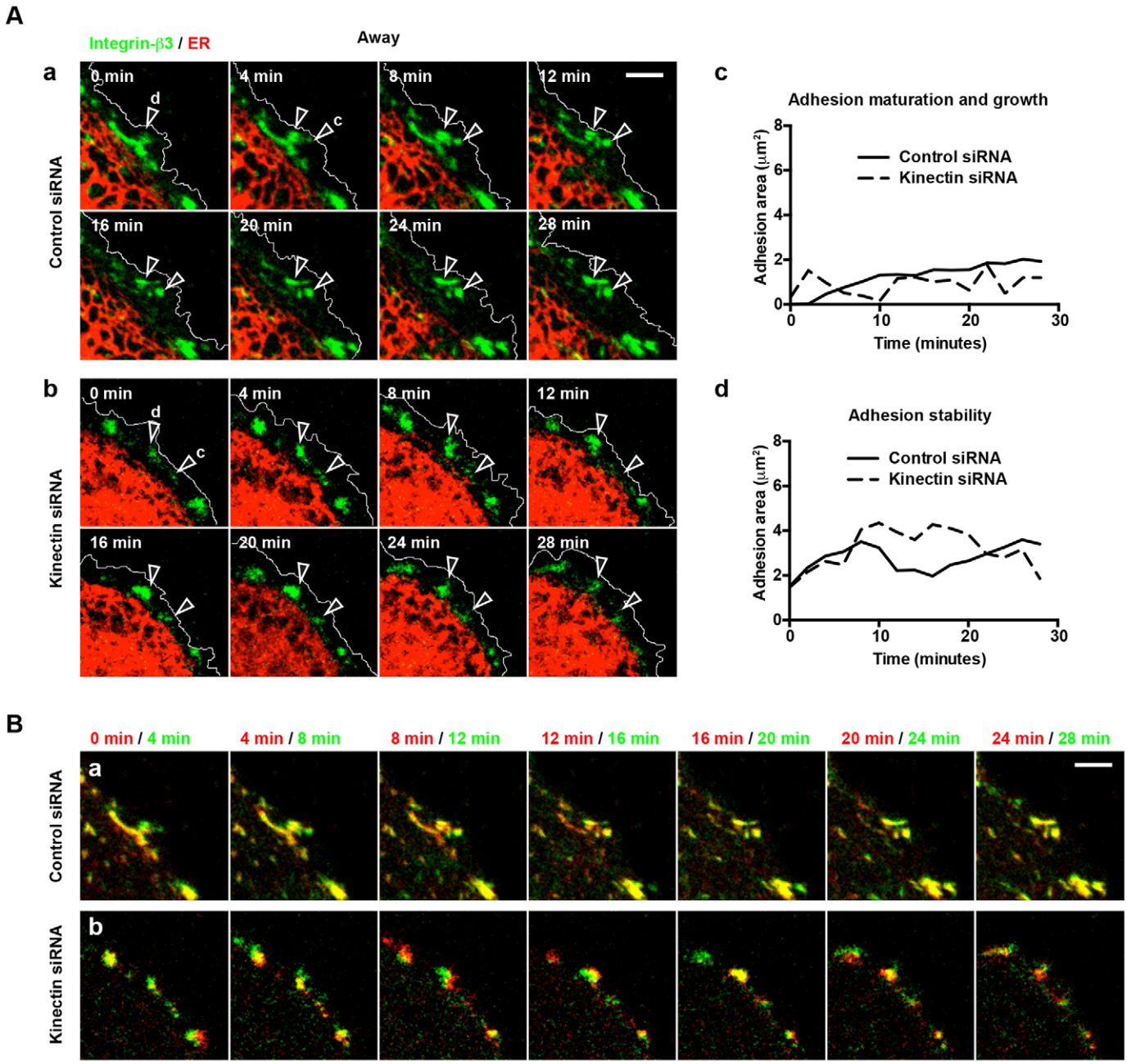

Fig. 7. Dynamics of ER and adhesions in protrusions oriented away from chemoattractant. (A) Time-lapse images showing protrusions oriented away from the chemoattractant during chemotaxis. Cells were transfected with integrin-β3–GFP (green) and pDsRed2-ER (red). Cell edges (white lines) were determined from DIC images. A micropipette with FBS was placed at the top left, ~250 µm away. ER was absent in protrusions oriented away from the chemoattractant of both control (a) and kinectin-knockdown cells (b). Focal complexes failed to mature into focal adhesions and the membrane did not extend forward. Arrowheads, adhesions without ER contact. Scale bar: 5 µm. (c,d) Quantification of the size of peripheral adhesions over time in a and b. Effects of focal complex maturation are represented as adhesion maturation and growth (c) and adhesion stability (d). (B) Timepoint overlays showing dynamics of integrin-β3–GFP adhesions in protrusions oriented away from the chemoattractant during chemotaxis. 'Current' and 'current+4 min' frames are colored red and green, respectively. Structures in green are new, structures in yellow are unchanged between frames and structures in red disassembled by the next frame. Scale bar: 5 µm.

(Arrieumerlou and Meyer, 2005) and in <10% (Bosgraaf et al., 2008). As we induced chemotaxis over a 1-mm bridge of a Dunn chamber, cells, which have a length of 67.6±26.0 µm (mean±s.d., n=89), were exposed to an average front-to-back difference in the concentration at the midpoint of the chamber of 6.76%. When the gradient was halved to 2.5–5% and 5–10% FBS gradients (Fig. S4), cells were exposed to an average front-to-back difference in the concentration at the midpoint of the chamber of 3.38%, which falls within the range of a shallow gradient as described by the other groups. We found that a 2.5–5% FBS gradient was not sufficient to elicit chemotaxis in MDA-MB-231 cells and that the migration behavior in 5–10% and 0–10% FBS gradients were the same, but the behavior in 0–10% FBS gradient was more robust and consistent.

Directional bias is mediated by directional sensing and polarization processes (Devreotes and Janetopoulos, 2003). Directional sensing appeared to be intact after knockdown of

Journal of Cell Science (2016) 129, 2660-2672 doi:10.1242/jcs.181768

kinectin, as cells attempted to polarize in response to the chemoattractant gradient through biased distribution of leading protrusions in the direction of the chemoattractant. However, the biased distribution of leading protrusions did not translate into directional migration in kinectin-knockdown cells, as preferential maintenance of these protrusions was impaired. Our results indicate the involvement of kinectin-dependent ER transport in the final steps of the polarization process. Cell protrusions are maintained by adhesion to the substratum; low adhesion strength results in unproductive protrusions, membrane ruffling and inefficient migration (Borm et al., 2005; Burridge and Wennerberg, 2004; Petrie et al., 2009). Focal complexes are tiny dot-like adhesions at the lamellipodia that generate strong propulsive traction during cell migration (Ballestrem et al., 2001; Beningo et al., 2001), whereas focal adhesions are slightly bigger oval adhesions at the cell lamella that provide strong adhesion to the substratum (Beningo et al., 2001; Zaidel-Bar et al., 2003; Zamir and Geiger, 2001). Consistent with the role of ER on adhesions (Zhang et al., 2010), we showed that ER contact promoted the maturation of focal complexes to focal adhesions. Protrusions oriented towards the chemoattractant had ER accumulation, thus were more likely to contain focal adhesions and be maintained than those oriented away. Our results provide a mechanism for the preferential maintenance of correctly oriented protrusions during chemotaxis in shallow gradients of chemoattractants, which was noted in a different study (Andrew and Insall, 2007).

Maturation of focal complexes to focal adhesions is impaired after knockdown of kinectin. Although chemotaxis was also affected, cells could still migrate with a similar velocity and persistence. Cell migration speed has a biphasic relationship with adhesion strength, with fast migration occurring at an intermediate adhesion strength, and slow migration occurring at both low and high adhesion strengths (Gupton and Waterman-Storer, 2006). MDA-MB-231 cells are a highly migratory metastatic breast cancer cell line that exhibit fast migration. Migrating MDA-MB-231 cells form focal adhesions with high turnover to enable fast migration (Urra et al., 2012). Therefore, decreased adhesion strength in kinectin-knockdown cells did not significantly increase migration speed. Our results suggest that focal complexes are sufficient to support cell migration of MDA-MB-231 cells. However, focal adhesions are still required for preferential maintenance of protrusions during directed migration such as chemotaxis.

The ER has been shown to mediate adhesion signaling through ER-bound proteins and intracellular Ca^{2+} release (English et al., 2009; Friedman and Voeltz, 2011). For example, protein-tyrosine phosphatase 1B (PTP1B, also known as PTPN1), an ER-bound protein, promotes focal complex maturation by targeting negative regulatory sites in Src (phosphorylated tyrosine 529), paxillin and p130Cas (also known as BCAR1) (Burdisso et al., 2013; Hernández et al., 2006). Meanwhile, Ca^{2+} release from the ER induced by interleukin 1β treatment promotes focal complex maturation in a SHP-2-dependent manner (Wang et al., 2006). Kinectin is a structural protein (Kumar et al., 1998; Yu et al., 1995) and rather than directly regulating cell adhesions, kinectin indirectly contributes by mediating ER transport to adhesion sites through kinesin-1 and MTs (Ong et al., 2000; Santama et al., 2004; Zhang et al., 2010).

MT polymerization is upstream of ER-dependent signaling, and controls access of ER to cellular regions because ER transport occurs along MTs (Terasaki et al., 1986). MTs are polarized during migration to support directional movement, and depolymerization of MTs with nocodazole abolishes chemotaxis (Ueda and Ogihara, 1994). The motor protein kinesin-1, which links kinectin and ER to MTs, preferentially moves on acetylated MTs (Friedman et al., 2010; Reed et al., 2006). Acetylation of MTs is a regulated modification that only occurs to a small fraction of MTs (Hubbert et al., 2002). During chemotaxis, MTs positioned in the direction of the leading edge are preferentially acetylated, possibly acting as the upstream signal that kinectin-dependent ER transport responds to. Hyperacetylation of MT results in enlarged focal adhesions (Tran et al., 2007), consistent with the role of kinectin-dependent ER transport. Kinectin–kinesin-1-dependent ER transport likely works in tandem with MT polarization and acetylation for preferential maintenance of correctly oriented protrusions during chemotaxis.

From our experience, ER retraction in kinectin-knockdown cells is most obvious during cell spreading and in regions with active membrane extension. Given enough time, after a cell reaches steady-state, the ER will still be distributed to the cell periphery, providing an explanation as to why ER retraction has not been observed in other studies (Plitz and Pfeffer, 2001; Shibata et al., 2010). This indicates that kinectin might be involved in kinesin-1-dependent fast ER transport to the cell periphery. The process might also be compensated for by other kinesin-1 interaction partners on the ER, such as ribosome receptor p180 (also known as RRBP1) (Diefenbach et al., 2004) and other motor proteins such as ER-bound myosin V (Tabb et al., 1998) and the slower TAC mechanism through STIM1 and EB1 (also known as MAPRE1) (Friedman et al., 2010; Grigoriev et al., 2008). Finally, static ER linkers such as CLIMP-63 (also known as CKAP4) and others might contribute to the retention of the peripheral ER, reducing ER retraction (Klopfenstein et al., 1998; Vedrenne et al., 2005; Vedrenne and Hauri, 2006).

In addition to kinesin-1 binding, kinectin also binds to elongation factor-1δ and a number of small G-proteins (Alberts et al., 1998; Hotta et al., 1996; Ong et al., 2003; Vignal et al., 2001). Elongation factor-1δ, which is involved in protein synthesis, has not been shown to have any effect on cell migration, although elongation factor-1 has been implicated in cancer cell invasion (Pecorari et al., 2009). However, we cannot rule out that it might indirectly contribute to the observed effects. By contrast, the small G-proteins Rac1, RhoA, Cdc42 and RhoG are well-studied signaling proteins in cell migration. Two-hybrid interaction studies have shown that activated forms of these small G-proteins interact strongly with kinectin, whereas inactivated forms do not, or only do so very weakly (Alberts et al., 1998; Hotta et al., 1996; Vignal et al., 2001). The role of kinectin in migration is in the transport of ER to the cell periphery where it promotes protrusion maintenance, but what signals recruit kinectin to transport ER to the leading edge requires further studies. Taken together, given that activation of small G-proteins are tightly controlled during cell migration and activated small G-proteins bind much more strongly to kinectin, activation of small G-proteins might be signaling molecules that recruit ER to cell periphery.

In summary, our results here propose a mechanism in which correctly orientated protrusions are stabilized and have consequent effects on chemotaxis in shallow gradient. Correctly oriented protrusions are stabilized by ER contact with focal complexes, which causes the maturation of focal complexes into focal adhesions, maintaining the protrusions. This mechanism allows cells to respond to chemoattractants and migrate towards it.

MATERIALS AND METHODS

Cell culture

An early passage MDA-MB-231 cell line from the ATCC was kindly provided by Hong Wanjin (Institute of Molecular and Cell Biology, Singapore). Subconfluent culture of MDA-MB-231 cells were maintained

Journal of Cell Science (2016) 129, 2660-2672 doi:10.1242/jcs.181768

in RPMI-1640 medium (Invitrogen) supplemented with 10% fetal bovine serum (FBS) (Invitrogen). Cells were maintained at 37°C in a humidified atmosphere with 5% CO_2.

siRNA treatment and plasmid transfection

The sense sequences of Stealth siRNA (Invitrogen) were as follows: human kinectin siRNA 5′-AGAAAAUGUCUUCGUAGAUGAACCC-3′; scrambled control siRNA 5′-AGAUAUGUCCUUGGAUAAGAAACCC-3′. Cells were treated with 40 nM siRNA using Lipofectamine RNAiMAX (Invitrogen) and OptiMEM medium (Invitrogen) according to the manufacturer's recommendation. Experiments were carried out at 48–96 h after siRNA treatment.

Integrin-β3–GFP, full-length mouse cDNA encoding integrin β3 and EGFP subcloned into pcDNA3, was kindly provided by Christoph Ballestrem (Faculty of Life Sciences, The University of Manchester, UK) (Ballestrem et al., 2001). The expression vector pDsRed2-ER encodes a fusion of *Discosoma sp.* red fluorescent protein (DsRed2) with the ER targeting and retention sequences. GFP–KNT^+ is a pEGFP-C1 vector with subcloned KNT^+ cDNA, whereas GFP^+ is an empty pEGFP vector used as a control (Santama et al., 2004). Both pEGFP and pDsRed2-ER vectors were purchased (Clontech Laboratories). Cells were transfected with the appropriate plasmids using Lipofectamine LTX (Invitrogen) and OptiMEM medium according to the manufacturer's recommendation. For knockdown studies, plasmid transfection was performed 24 h after siRNA treatment. Experiments were carried out 24–72 h after transfection.

Antibodies, immunofluorescence staining and western blotting

The following primary antibodies were used: rabbit anti-kinectin (sc-33562; western blotting 1:750, immunofluorescence staining 1:133; Santa Cruz Biotechnology), mouse anti-β-actin (western blotting 1:10,000), mouse anti-vinculin (V9264; 1:133), and rabbit anti-PDI (P7372; 1:133) (all Sigma-Aldrich). For secondary antibodies, donkey anti-rabbit-IgG conjugated to Alexa Fluor 488 (1:200) and donkey anti-mouse-IgG conjugated to Alexa Fluor 546 (1:200) (Invitrogen) were used for immunofluorescence staining, whereas rabbit anti-mouse-IgG conjugated to horseradish peroxidase (HRP) (1:10,000) and goat anti-rabbit-IgG conjugated to HRP (1:40,000) (Sigma-Aldrich) were used for western blotting. Phalloidin–Alexa-Fluor-633 (1:75; Invitrogen) was used in conjunction with secondary antibodies for immunofluorescence staining of actin filaments.

For immunofluorescence staining, cells cultured on fibronectin-coated glass coverslips were fixed with 3.7% paraformaldehyde (PFA) for 10 min at 37°C and then permeabilized with 0.1% Triton X-100 for 10 min at room temperature. Fixed cells were blocked with 1% bovine serum albumin (BSA) (Sigma-Aldrich) in phosphate-buffered saline (PBS) for 1 h at room temperature, before incubation with the appropriate primary antibodies for 2 h at room temperature. Cells were then washed and incubated for 1 h at room temperature with the appropriate secondary antibodies. Finally, coverslips were washed and mounted in Fluorescent Mounting Medium (Dako, Glostrup, Denmark) on glass slides.

For western blotting, the total protein was isolated with RIPA buffer. The protein concentration of the supernatant was determined using a DC Protein Assay (Bio-Rad). Equal concentrations of protein extracts were electrophoretically resolved on SDS-polyacrylamide gels and transferred to 0.45-µm nitrocellulose membranes (Bio-Rad). Membranes were blocked with 5% skim milk (Bio-Rad) for 1 h at room temperature and incubated with the appropriate primary and secondary antibodies. β-actin was used as an internal control. Detection was performed using SuperSignal West Pico Chemiluminescent Substrate (Thermo Scientific).

Migration assays

Transwell chemotaxis assays were performed in 24-well plates using 12-mm Millicell-PCF inserts with a membrane pore size of 8.0 µm (Millipore). A porous membrane separates the upper compartment of the insert containing RPMI-1640 basal medium from the lower compartment containing growth medium. A total of 5×10^4 MDA-MB-231 cells were seeded into the upper compartment, onto the top membrane surface. Cells were allowed to migrate to the bottom membrane surface facing the lower compartment, towards a 10% FBS gradient for 3 h. Afterwards, cells were fixed with 3.7% PFA. Cells remaining on the top membrane surface were wiped off and cells on the bottom membrane surface were stained with Trypan Blue (Invitrogen). Images of the bottom membrane surface were acquired with an IX70 inverted microscope (Olympus, Shinjuku, Japan) using a 10×/0.25 NA LWD C Plan HMC objective (Modulation Optics, Rochester, NY). Cell migration was presented as the mean number of cells per field. At least 20 random fields were quantified for each insert and three independent experiments were performed.

For wound healing assays, cells were seeded in 24-well plates and cultured to confluence overnight. The confluent monolayer was scraped using a pipette tip to form a wound. Cells adjacent to the wound were allowed to migrate into the wound. Images along the wound were captured immediately and 4 h after wounding with an IX70 inverted microscope using 10×/0.25 NA LWD C Plan HMC objective. The wound area was measured using ImageJ software (NIH). Cell migration was presented as the rate of wound closure.

Fibronectin coating of glass surfaces

Glass-bottom dishes (MatTek), square-gridded photoetched coverslips (Electron Microscopy Sciences, Hatfield, UK) and glass coverslips (Menzel-Gläser, Braunschweig, Germany) were acid washed with 10 M nitric acid for 1 h and thoroughly rinsed five times in PBS for 10 min each before being coated with 10 µg/ml fibronectin. After coating, glass surfaces were rinsed once again with PBS before cells were seeded.

Random migration assays

MDA-MB-231 cells were seeded on fibronectin-coated glass-bottom dishes at a density of 1000 cells/cm^2 and allowed to attach overnight. Existing medium was replaced with fresh growth medium before live-cell imaging. Cells were maintained in a humidified chamber in the presence of 5% CO_2 at 37°C and imaged at 10-min intervals for 8 h with FV1000 microscopes (Olympus) using a 10×/0.35 NA Plan Apo or 10×/0.35 NA UPlan Apo objective (Olympus). Cell coordinates over time were tracked with Metamorph software (Molecular Devices). The velocity and persistence of migration were calculated from the set of coordinates with the Chemotaxis and Migration Tool (ibidi).

Dunn chamber assays

Chemotaxis experiments were performed in a Dunn chamber (Hawksley, Sussex, UK). MDA-MB-231 cells were seeded on fibronectin-coated glass coverslips and allowed to attach overnight. Cells were maintained in basal medium for 4 h before the glass coverslip was assembled on the Dunn chamber. The inner well was filled with basal medium while the outer well was filled with 10% FBS growth medium. The glass coverslip was sealed in place with hot wax mixture (vaseline, paraffin and beeswax, 1:1:1). The chamber was then maintained at 37°C and imaged at 10-min intervals for 12 h with FV1000 microscope using a 10×/0.35 NA UPlan Apo objective. Cell coordinates over time were tracked with Metamorph software. Parameters of cell migration were calculated from the set of coordinates with the Chemotaxis and Migration Tool.

For live imaging of ER dynamics, the experimental method was slightly modified, with additional steps after maintenance in basal medium. Cells were further incubated with 1 µg/ml ER Tracker Blue-White DPX (Invitrogen) in basal medium for 30 min. Glass coverslips were then washed with growth medium and assembled on a Dunn chamber.

For immunofluorescence staining of cells undergoing chemotaxis, MDA-MB-231 cells were seeded on a fibronectin-coated square-gridded photoetched glass coverslip and were allowed to attach overnight. Cells were maintained in basal medium for 4 h before the glass coverslip was assembled on the Dunn chamber. After assembly, grid positions of the glass coverslip corresponding to the bridge of the Dunn chamber, where chemotaxis occurs, were mapped and imaged with an FV1000 microscope and 10×/0.35 NA UPlan Apo objective (Olympus). Cells were then allowed to undergo chemotaxis for 6 h at 37°C. Following that, the Dunn chamber was carefully disassembled in a warm environment and cells were immediately fixed with warm 3.7% PFA for immunofluorescence

staining. Before confocal imaging of immunolabeled cells, images of the glass coverslip overlaying the bridge of the Dunn chamber from the previous step were first assembled with the MosiacJ plugin of ImageJ (Thévenaz and Unser, 2007). The mosaic image was used to establish the position and orientation of the bridge on the glass coverslip. Immunolabeled cells at the bridge were located with an FV1000 microscope and 10×/0.35 NA UPlan Apo objective, and images were captured with a 60×/1.45 NA Plan Apo OTIRFM objective.

Kymographs

The Dunn chamber was assembled using the method described for cell tracking. TIRF time-lapse images taken at 1-s intervals for 10 min were acquired with a FV1000 microscope with a 60×/1.45 NA Plan Apo OTIRFM objective (Olympus) and captured with a CoolSNAP HQ2 camera (Photometrics, Tucson, AZ). Kymographs of leading edges were produced and analyzed using ImageJ software by lining up 1-pixel-wide regions in the direction of edge movement on a time scale. The resulting composite picture was used for quantification of the velocity, amplitude and frequency of lamellipodia movement.

Micropipette chemotaxis assays

MDA-MB-231 cells co-transfected with integrin-β3–GFP and pDsRed2-ER were seeded on glass-bottom dishes. Cells were maintained for 4 h in RPMI-1640 medium with 2% FBS prior to the assay. Assays were conducted in a humidified chamber in presence of 5% CO_2 at 37°C. Chemotaxis was induced with a Femtotip loaded with 100% FBS and maintained at positive pressure of 25 psi at a distance of 150 to 300 µm from the cell. Positioning and pressure of Femtotip were respectively controlled using Micromanipulator 5171 and Transjector 5246 (Eppendorf, Hamburg, Germany). Cells migrating towards the tip were imaged with a FV1000 microscope and 60×/1.45 NA Plan Apo OTIRFM or 60×/1.35 NA UPlanS Apo O objective (Olympus) at 1-min intervals for 90 min.

Image processing and analysis

For quantification of adhesion area, images of vinculin staining were first processed with the high bandpass filter and threshold plugins of ImageJ to remove background signals. Subsequently, adhesion plaques with an area >1 μm^2 within leading edges were measured using the Analyze Particles plugin. Adhesion areas were normalized to peripheral lengths of leading edges that were determined from images of actin staining. All measured values were sorted according to orientation towards the chemoattractant.

Acknowledgements

We thank the professional support from the staff of the NUHS core facilities for help with confocal microscopy and flow cytometry.

Competing interests

The authors declare no competing or financial interests.

Author contributions

I.C.N. designed and performed the experiments, analyzed the data and prepared the manuscript; P.P. analyzed the data and prepared the manuscript; L.Y.T. performed the experiments and analyzed data; H.L. analyzed the data; S.Y.L. designed the experiments; H.Y. designed the experiments and prepared the manuscript.

Funding

This work is supported in part by funding from the Mechanobiology Institute, Singapore (MBI); National Medical Research Council (Cooperative Basic Research Grant); Institute of Bioengineering and Nanotechnology, Singapore (IBN); Biomedical Research Council, Singapore (BMRC); A*STAR Joint Council Development Programme (JCO-DP) (Project Number 1334i00051); Ministry of Education - Singapore; and the Singapore-MIT Alliance Research and Technology (SMART-BioSyM). I.C.N. and P.P. are NUS Graduate School for Integrative Sciences and Engineering (NGS) scholars.

Supplementary information

Supplementary information available online at
http://jcs.biologists.org/lookup/doi/10.1242/jcs.181768.supplemental

References

Alberts, A. S., Bouquin, N., Johnston, L. H. and Treisman, R. (1998). Analysis of RhoA-binding proteins reveals an interaction domain conserved in heterotrimeric G protein beta subunits and the yeast response regulator protein Skn7. *J. Biol. Chem.* **273**, 8616-8622.

Andrew, N. and Insall, R. H. (2007). Chemotaxis in shallow gradients is mediated independently of PtdIns 3-kinase by biased choices between random protrusions. *Nat. Cell Biol.* **9**, 193-200.

Arrieumerlou, C. and Meyer, T. (2005). A local coupling model and compass parameter for eukaryotic chemotaxis. *Dev. Cell* **8**, 215-227.

Ballestrem, C., Hinz, B., Imhof, B. A. and Wehrle-Haller, B. (2001). Marching at the front and dragging behind: differential alphaVbeta3-integrin turnover regulates focal adhesion behavior. *J. Cell Biol.* **155**, 1319-1332.

Beningo, K. A., Dembo, M., Kaverina, I., Small, J. V. and Wang, Y.-l. (2001). Nascent focal adhesions are responsible for the generation of strong propulsive forces in migrating fibroblasts. *J. Cell Biol.* **153**, 881-888.

Borm, B., Requardt, R. P., Herzog, V. and Kirfel, G. (2005). Membrane ruffles in cell migration: indicators of inefficient lamellipodia adhesion and compartments of actin filament reorganization. *Exp. Cell Res.* **302**, 83-95.

Bosgraaf, L., Keizer-Gunnink, I. and Van Haastert, P. J. (2008). PI3-kinase signaling contributes to orientation in shallow gradients and enhances speed in steep chemoattractant gradients. *J. Cell Sci.* **121**, 3589-3597.

Burdisso, J. E., Gonzalez, A. and Arregui, C. O. (2013). PTP1B promotes focal complex maturation, lamellar persistence and directional migration. *J. Cell Sci.* **126**, 1820-1831.

Burridge, K. and Wennerberg, K. (2004). Rho and Rac take center stage. *Cell* **116**, 167-179.

Devreotes, P. and Janetopoulos, C. (2003). Eukaryotic chemotaxis: distinctions between directional sensing and polarization. *J. Biol. Chem.* **278**, 20445-20448.

Devreotes, P. N. and Zigmond, S. H. (1988). Chemotaxis in eukaryotic cells: a focus on leukocytes and Dictyostelium. *Annu. Rev. Cell Biol.* **4**, 649-686.

Diefenbach, R. J., Diefenbach, E., Douglas, M. W. and Cunningham, A. L. (2004). The ribosome receptor, p180, interacts with kinesin heavy chain, KIF5B. *Biochem. Biophys. Res. Commun.* **319**, 987-992.

English, A. R., Zurek, N. and Voeltz, G. K. (2009). Peripheral ER structure and function. *Curr. Opin. Cell Biol.* **21**, 596-602.

Friedman, J. R. and Voeltz, G. K. (2011). The ER in 3D: a multifunctional dynamic membrane network. *Trends Cell Biol.* **21**, 709-717.

Friedman, J. R., Webster, B. M., Mastronarde, D. N., Verhey, K. J. and Voeltz, G. K. (2010). ER sliding dynamics and ER–mitochondrial contacts occur on acetylated microtubules. *J. Cell Biol.* **190**, 363-375.

Grigoriev, I., Gouveia, S. M., van der Vaart, B., Demmers, J., Smyth, J. T., Honnappa, S., Splinter, D., Steinmetz, M. O., Putney, J. W., Jr., Hoogenraad, C. C. et al. (2008). STIM1 is a MT-plus-end-tracking protein involved in remodeling of the ER. *Curr. Biol.* **18**, 177-182.

Gupton, S. L. and Waterman-Storer, C. M. (2006). Spatiotemporal feedback between actomyosin and focal-adhesion systems optimizes rapid cell migration. *Cell* **125**, 1361-1374.

Harms, B. D., Bassi, G. M., Horwitz, A. R. and Lauffenburger, D. A. (2005). Directional persistence of EGF-induced cell migration is associated with stabilization of lamellipodial protrusions. *Biophys. J.* **88**, 1479-1488.

Hernández, M. V., Sala, M. G. D., Balsamo, J., Lilien, J. and Arregui, C. O. (2006). ER-bound PTP1B is targeted to newly forming cell-matrix adhesions. *J. Cell Sci.* **119**, 1233-1243.

Hotta, K., Tanaka, K., Mino, A., Kohno, H. and Takai, Y. (1996). Interaction of the Rho family small G proteins with kinectin, an anchoring protein of kinesin motor. *Biochem. Biophys. Res. Commun.* **225**, 69-74.

Hubbert, C., Guardiola, A., Shao, R., Kawaguchi, Y., Ito, A., Nixon, A., Yoshida, M., Wang, X.-F. and Yao, T.-P. (2002). HDAC6 is a microtubule-associated deacetylase. *Nature* **417**, 455-458.

Klopfenstein, D. R., Kappeler, F. and Hauri, H.-P. (1998). A novel direct interaction of endoplasmic reticulum with microtubules. *EMBO J.* **17**, 6168-6177.

Kumar, J., Yu, H. and Sheetz, M. P. (1995). Kinectin, an essential anchor for kinesin-driven vesicle motility. *Science* **267**, 1834-1837.

Kumar, J., Erickson, H. P. and Sheetz, M. P. (1998). Ultrastructural and biochemical properties of the 120-kDa form of chick kinectin. *J. Biol. Chem.* **273**, 31738-31743.

Lauffenburger, D. A. and Horwitz, A. F. (1996). Cell migration: a physically integrated molecular process. *Cell* **84**, 359-369.

Ong, L.-L., Lim, A. P. C., Er, C. P. N., Kuznetsov, S. A. and Yu, H. (2000). Kinectin-kinesin binding domains and their effects on organelle motility. *J. Biol. Chem.* **275**, 32854-32860.

Ong, L.-L., Er, C. P. N., Ho, A., Aung, M. T. and Yu, H. (2003). Kinectin anchors the translation elongation factor-1 delta to the endoplasmic reticulum. *J. Biol. Chem.* **278**, 32115-32123.

Pankov, R., Endo, Y., Even-Ram, S., Araki, M., Clark, K., Cukierman, E., Matsumoto, K. and Yamada, K. M. (2005). A Rac switch regulates random versus directionally persistent cell migration. *J. Cell Biol.* **170**, 793-802.

Pecorari, L., Marin, O., Silvestri, C., Candini, O., Rossi, E., Guerzoni, C., Cattelani, S., Mariani, S. A., Corradini, F., Ferrari-Amorotti, G. et al. (2009).

Elongation Factor 1 alpha interacts with phospho-Akt in breast cancer cells and regulates their proliferation, survival and motility. *Mol. Cancer* **8**, 58.
Petrie, R. J., Doyle, A. D. and Yamada, K. M. (2009). Random versus directionally persistent cell migration. *Nat. Rev. Mol. Cell Biol.* **10**, 538-549.
Plitz, T. and Pfeffer, K. (2001). Intact lysosome transport and phagosome function despite kinectin deficiency. *Mol Cell Biol* **21**, 6044-6055.
Pollard, T. D. and Borisy, G. G. (2003). Cellular motility driven by assembly and disassembly of actin filaments. *Cell* **112**, 453-465.
Reed, N. A., Cai, D., Blasius, T. L., Jih, G. T., Meyhofer, E., Gaertig, J. and Verhey, K. J. (2006). Microtubule acetylation promotes kinesin-1 binding and transport. *Curr. Biol.* **16**, 2166-2172.
Ridley, A. J., Schwartz, M. A., Burridge, K., Firtel, R. A., Ginsberg, M. H., Borisy, G., Parsons, J. T. and Horwitz, A. R. (2003). Cell migration: integrating signals from front to back. *Science* **302**, 1704-1709.
Santama, N., Er, C. P., Ong, L.-L. and Yu, H. (2004). Distribution and functions of kinectin isoforms. *J. Cell Sci.* **117**, 4537-4549.
Shibata, Y., Shemesh, T., Prinz, W. A., Palazzo, A. F., Kozlov, M. M. and Rapoport, T. A. (2010). Mechanisms determining the morphology of the peripheral ER. *Cell* **143**, 774-788.
Swaney, K. F., Huang, C.-H. and Devreotes, P. N. (2010). Eukaryotic chemotaxis: a network of signaling pathways controls motility, directional sensing, and polarity. *Annu. Rev. Biophys.* **39**, 265-289.
Tabb, J. S., Molyneaux, B. J., Cohen, D. L., Kuznetsov, S. A. and Langford, G. M. (1998). Transport of ER vesicles on actin filaments in neurons by myosin V. *J. Cell Sci.* **111**, 3221-3234.
Terasaki, M., Chen, L. B. and Fujiwara, K. (1986). Microtubules and the endoplasmic reticulum are highly interdependent structures. *J. Cell Biol.* **103**, 1557-1568.
Thévenaz, P. and Unser, M. (2007). User-friendly semiautomated assembly of accurate image mosaics in microscopy. *Microsc. Res. Tech.* **70**, 135-146.
Toyoshima, I., Yu, H., Steuer, E. R. and Sheetz, M. P. (1992). Kinectin, a major kinesin-binding protein on ER. *J. Cell Biol.* **118**, 1121-1131.
Tran, A. D.-A., Marmo, T. P., Salam, A. A., Che, S., Finkelstein, E., Kabarriti, R., Xenias, H. S., Mazitschek, R., Hubbert, C., Kawaguchi, Y. et al. (2007). HDAC6 deacetylation of tubulin modulates dynamics of cellular adhesions. *J. Cell Sci.* **120**, 1469-1479.
Ueda, M. and Ogihara, S. (1994). Microtubules are required in amoeba chemotaxis for preferential stabilization of appropriate pseudopods. *J. Cell Sci.* **107**, 2071-2079.
Urra, H., Torres, V. A., Ortiz, R. J., Lobos, L., Díaz, M. I., Díaz, N., Härtel, S., Leyton, L. and Quest, A. F. G. (2012). Caveolin-1-enhanced motility and focal adhesion turnover require tyrosine-14 but not accumulation to the rear in metastatic cancer cells. *PLoS ONE* **7**, e33085.
Vedrenne, C. and Hauri, H.-P. (2006). Morphogenesis of the endoplasmic reticulum: beyond active membrane expansion. *Traffic* **7**, 639-646.
Vedrenne, C., Klopfenstein, D. R. and Hauri, H. P. (2005). Phosphorylation controls CLIMP-63-mediated anchoring of the endoplasmic reticulum to microtubules. *Mol. Biol. Cell* **16**, 1928-1937.
Vignal, E., Blangy, A., Martin, M., Gauthier-Rouviere, C. and Fort, P. (2001). Kinectin is a key effector of RhoG microtubule-dependent cellular activity. *Mol. Cell. Biol.* **21**, 8022-8034.
Wang, Q., Herrera Abreu, M. T., Siminovitch, K., Downey, G. P. and McCulloch, C. A. (2006). Phosphorylation of SHP-2 regulates interactions between the endoplasmic reticulum and focal adhesions to restrict interleukin-1-induced Ca2+ signaling. *J. Biol. Chem.* **281**, 31093-31105.
Waterman-Storer, C. M. and Salmon, E. D. (1998). Endoplasmic reticulum membrane tubules are distributed by microtubules in living cells using three distinct mechanisms. *Curr. Biol.* **8**, 798-807.
Wozniak, M. J., Bola, B., Brownhill, K., Yang, Y.-C., Levakova, V. and Allan, V. J. (2009). Role of kinesin-1 and cytoplasmic dynein in endoplasmic reticulum movement in VERO cells. *J. Cell Sci.* **122**, 1979-1989.
Yang, S., Zhang, J. J. and Huang, X.-Y. (2009). Orai1 and STIM1 are critical for breast tumor cell migration and metastasis. *Cancer Cell* **15**, 124-134.
Yu, H., Nicchitta, C. V., Kumar, J., Becker, M., Toyoshima, I. and Sheetz, M. P. (1995). Characterization of kinectin, a kinesin-binding protein: primary sequence and N-terminal topogenic signal analysis. *Mol. Biol. Cell* **6**, 171-183.
Zaidel-Bar, R., Ballestrem, C., Kam, Z. and Geiger, B. (2003). Early molecular events in the assembly of matrix adhesions at the leading edge of migrating cells. *J. Cell Sci.* **116**, 4605-4613.
Zamir, E. and Geiger, B. (2001). Molecular complexity and dynamics of cell-matrix adhesions. *J. Cell Sci.* **114**, 3583-3590.
Zhang, X., Tee, Y. H., Heng, J. K., Zhu, Y., Hu, X., Margadant, F., Ballestrem, C., Bershadsky, A., Griffiths, G. and Yu, H. (2010). Kinectin-mediated endoplasmic reticulum dynamics supports focal adhesion growth in the cellular lamella. *J. Cell Sci.* **123**, 3901-3912.

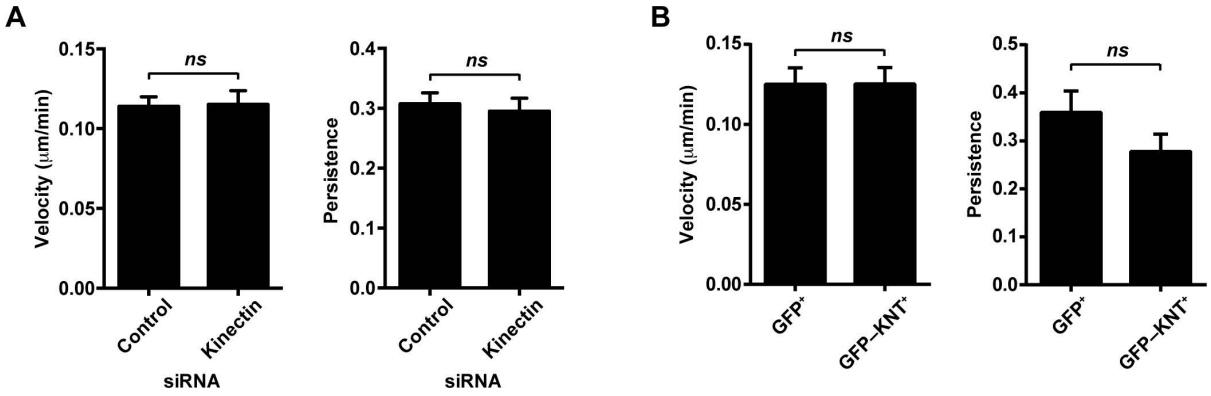

Figure S1| The velocity and persistence of migration during chemotaxis after kinectin knockdown and KNT$^+$ expression. (A) After kinectin knockdown, the velocity (control siRNA, 0.114 ± 0.006 μm/min; kinectin siRNA, 0.115 ± 0.009 μm/min; $p = 0.14$) and persistence of migration (control siRNA, 0.307 ± 0.018; kinectin siRNA, 0.295 ± 0.022; $p = 0.32$) were unaffected. **(B)** After KNT$^+$ expression, the velocity (GFP$^+$, 0.125 ± 0.010 μm/min; GFP–KNT$^+$, 0.125 ± 0.010 μm/min; $p = 0.91$) and persistence of migration (GFP$^+$, 0.359 ± 0.044; GFP–KNT$^+$, 0.278 ± 0.036; $p = 0.43$) were unaffected. Error bars represent s.e.m. *ns*, not significant; unpaired Student's *t* test.

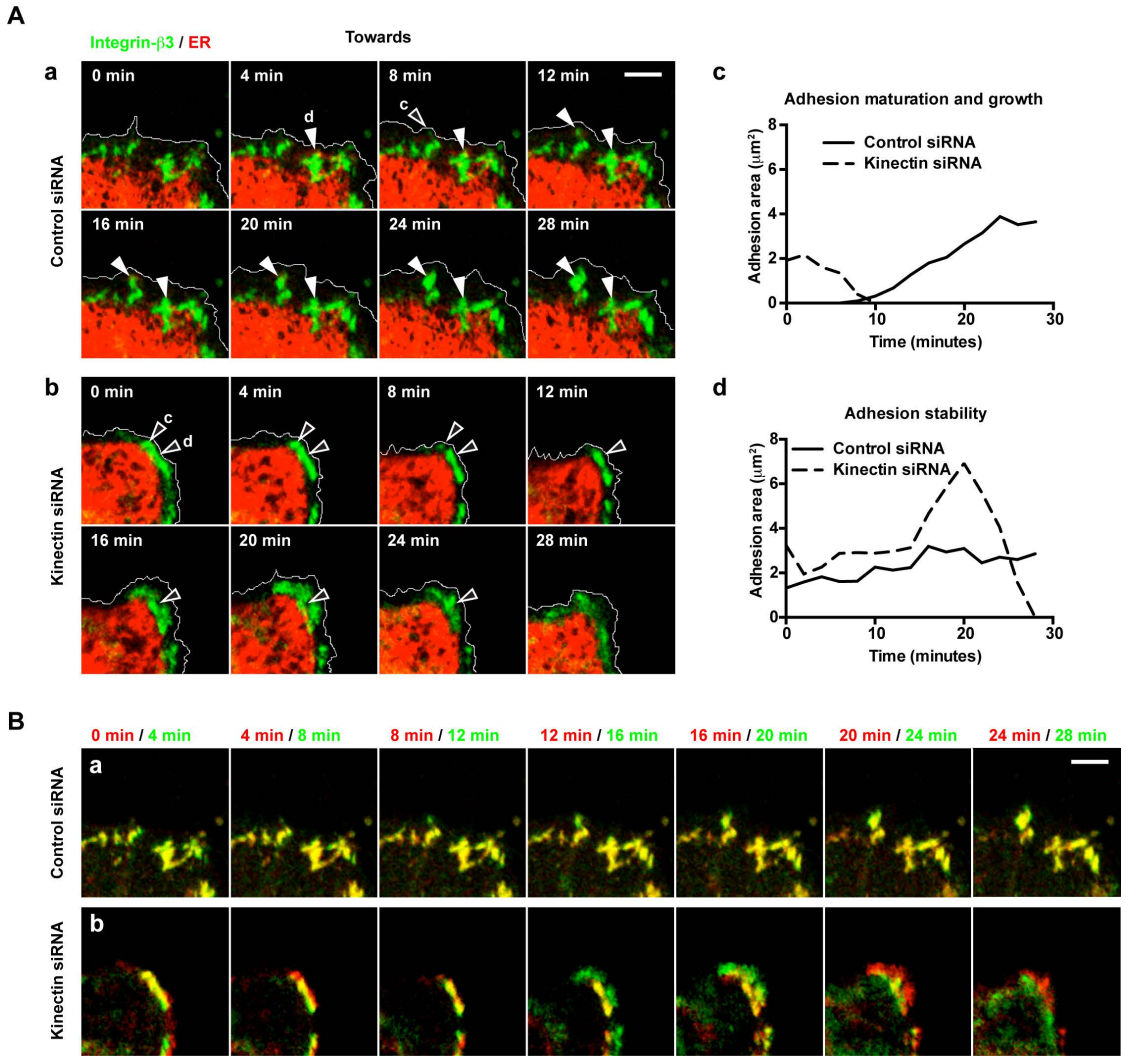

Fig. S2| Additional example showing the dynamics of ER and adhesions in protrusions oriented towards the chemoattractant. (A) Timelapse images show the dynamics of protrusions oriented towards the chemoattractant during chemotaxis. Cells were transfected with integrin β3–GFP (green) and pDsRed2–ER (red). Cell edges (white lines) were determined from DIC images. Micropipette with FBS was placed at top direction about 200 μm away. *Filled arrows*, adhesions with ER contact; *empty arrows*, adhesions without ER contact. Scale bar: 5 μm. Quantification of adhesions over time in (a) and (b) are also shown, with changes represented as adhesion maturation and growth (c) and adhesion stability (d). **(B)** Timepoint overlays show dynamics of integrin β3–GFP adhesions in protrusions oriented towards the chemoattractant during chemotaxis. 'Current' and 'current + 4 minutes' frames are colored red and green, respectively. Structures in green are new; structures in yellow are unchanged between frames while structures in red disassembled by the next frame. Scale bar: 5 μm.

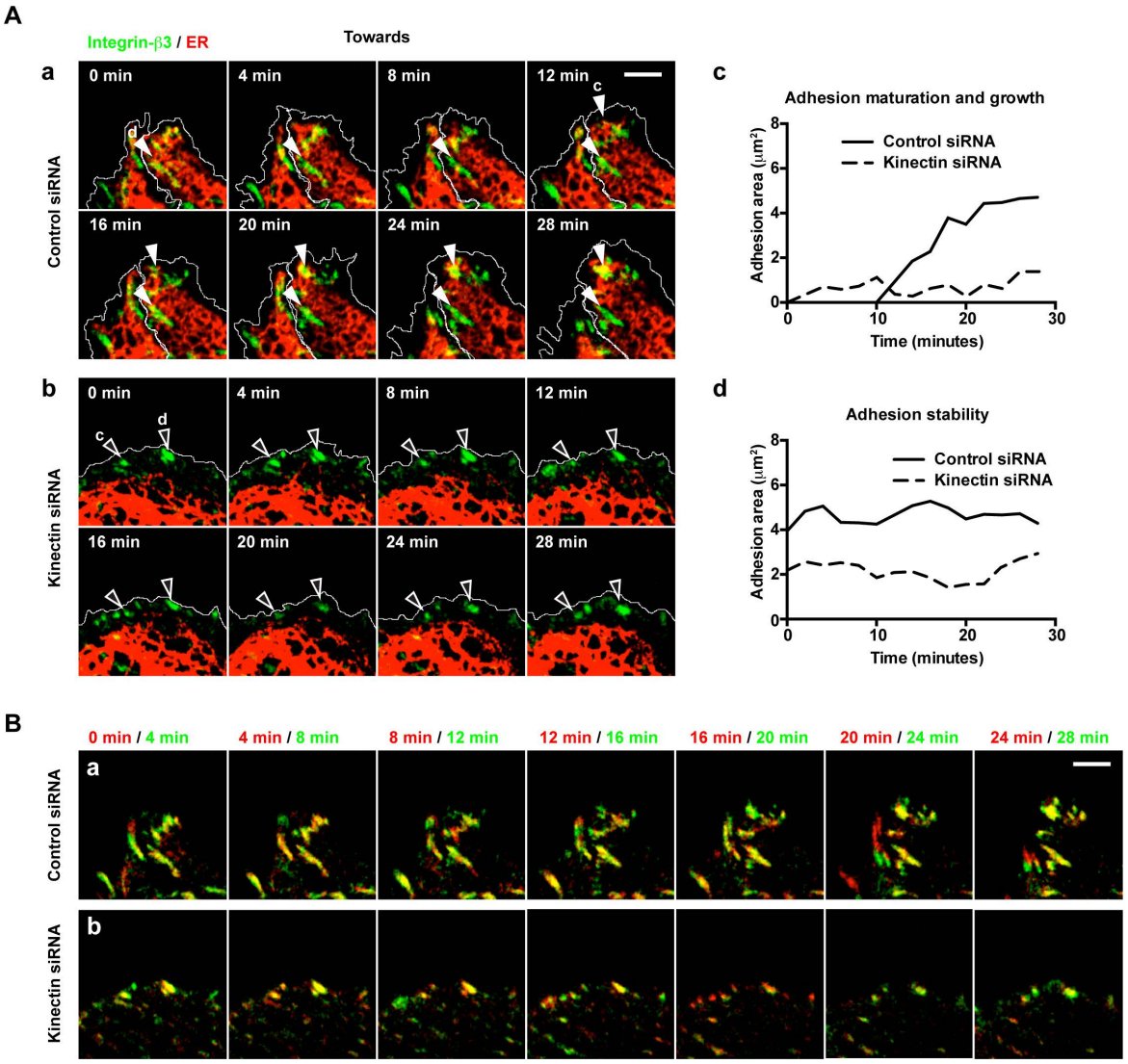

Fig. S3| Additional example showing the dynamics of ER and adhesions in protrusions oriented towards the chemoattractant. (A) Timelapse images show the dynamics of protrusions oriented towards the chemoattractant during chemotaxis. Cells were transfected with integrin β3–GFP (green) and pDsRed2–ER (red). Cell edges (white lines) were determined from DIC images. Micropipette with FBS was placed at top direction about 200 μm away. *Filled arrows*, adhesions with ER contact; *empty arrows*, adhesions without ER contact. Scale bar: 5 μm. Quantification of adhesions over time in (a) and (b) are also shown, with changes represented as adhesion maturation and growth (c) and adhesion stability (d). **(B)** Timepoint overlays show dynamics of integrin β3–GFP adhesions in protrusions oriented towards the chemoattractant during chemotaxis. 'Current' and 'current + 4 minutes' frames are colored red and green, respectively. Structures in green are new; structures in yellow are unchanged between frames while structures in red disassembled by the next frame. Scale bar: 5 μm.

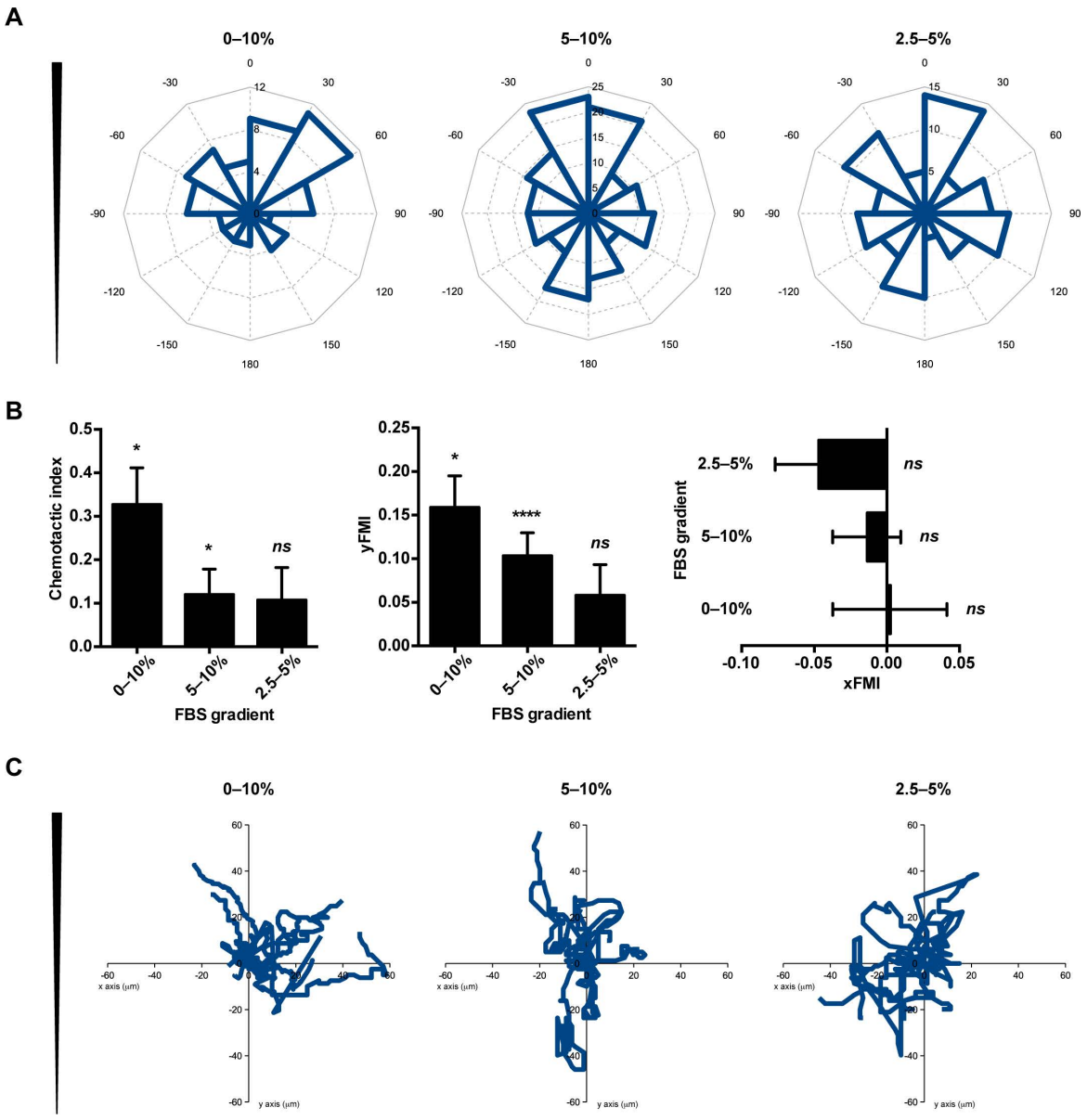

Fig. S4| Chemotaxis of MDA-MB-231 cells in different chemoattractant gradients. (A) MDA-MB-231 cells were allowed to migrate in 0–10%, 5–10% and 2.5–5% FBS gradients. Rose plots show that the cell migration in 0–10% and 5–10% but not 2.5–5% gradient was directionally biased. Direction of the chemoattractant gradient is towards the top. Cells were imaged in Dunn chamber at 10-minute intervals over a 12-hour period. A total of 60 cells for 0–10% gradient, 161 cells for 5–10% gradient and 92 cells for 2.5–5% gradient were quantified. **(B)** Chemotactic index and yFMI were significant for 0–10% and 5–10% gradients but not 2.5–5% gradient. The xFMI was not significant for all gradients tested. Error bars represent s.e.m. *ns*, not significant; *, $p < 0.05$; ****, $p < 0.0001$; column statistics, hypothetical value = 0.00. **(C)** Migration tracks in different chemoattractant gradients.

Movie S1| Migration of control cells in uniform chemoattractant gradient. Cells were allowed to migrate on fibronectin-coated glass-bottom dish in growth media.

Movie S2| Migration of kinectin knockdown cells in uniform chemoattractant gradient. Cells were allowed to migrate on fibronectin-coated glass-bottom dish in growth media.

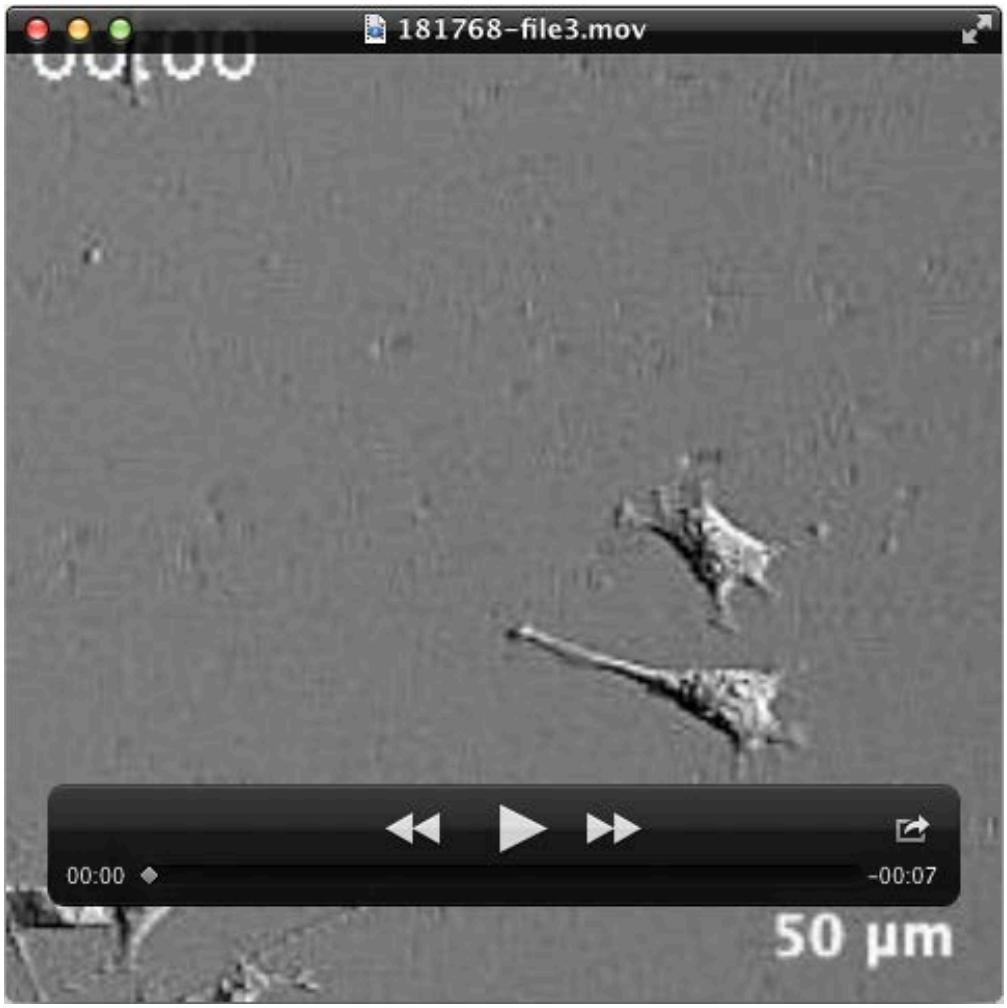

Movie S3| Migration of control cells in during chemotaxis in shallow gradients. Cells were allowed to migrate towards 10% FBS in Dunn chamber. Direction of chemoattractant gradient is towards the top.

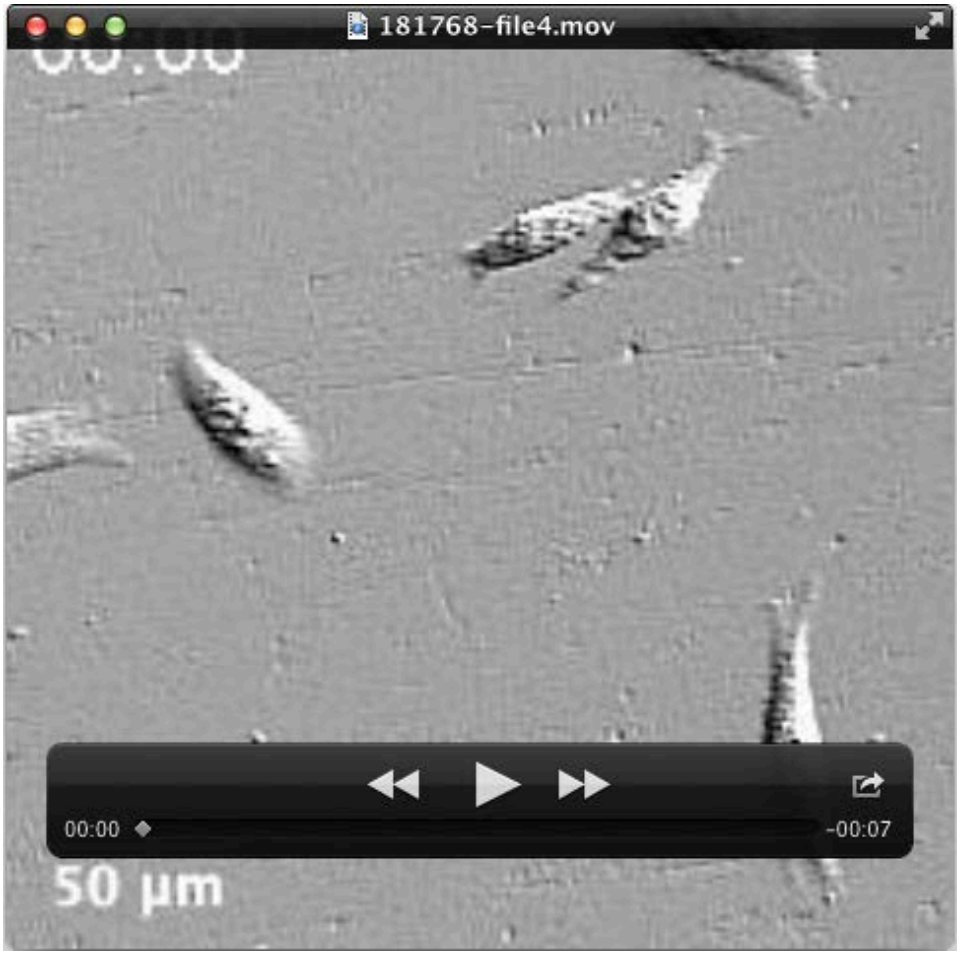

Movie S4| Migration of kinectin knockdown cells in during chemotaxis in shallow gradients. Cells were allowed to migrate towards 10% FBS in Dunn chamber. Direction of chemoattractant gradient is towards the top.

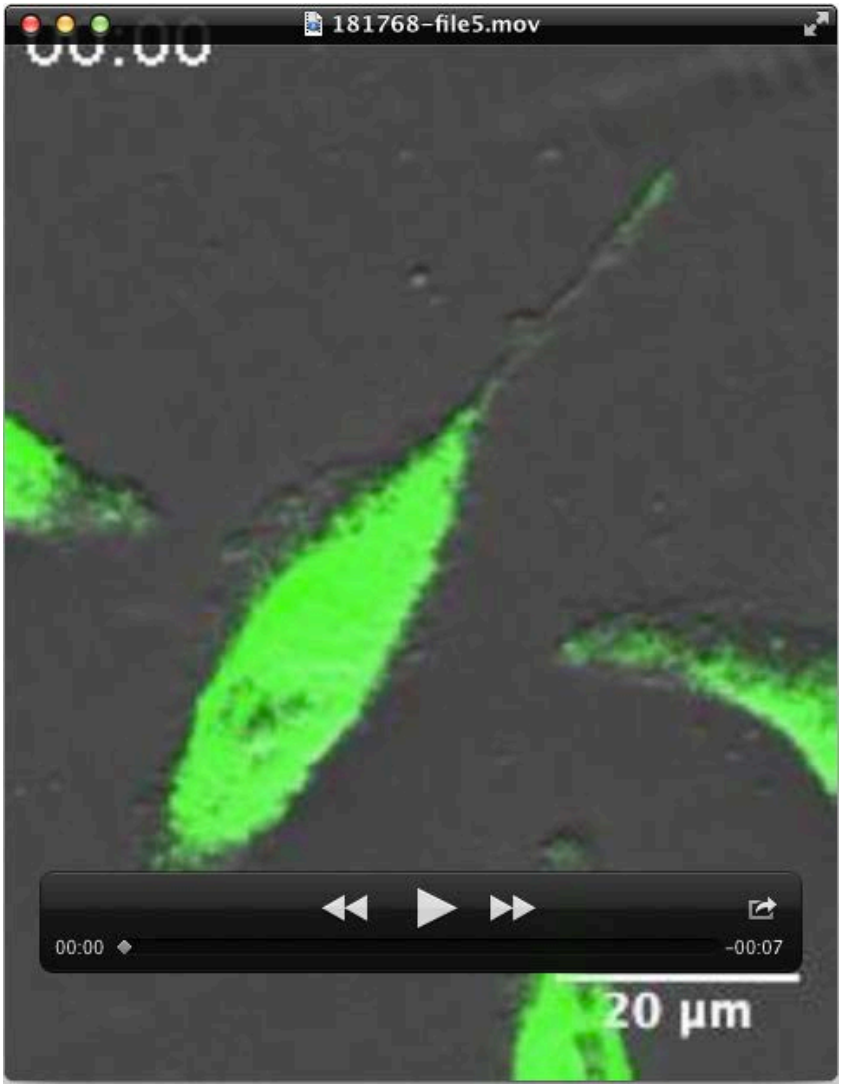

Movie S5| Dynamics of ER between opposing protrusions. MDA-MB-231 cells were stained with ER Tracker Blue-White DPX and were allowed to migrate towards 10% FBS in Dunn chamber. Direction of chemoattractant gradient is towards the top.

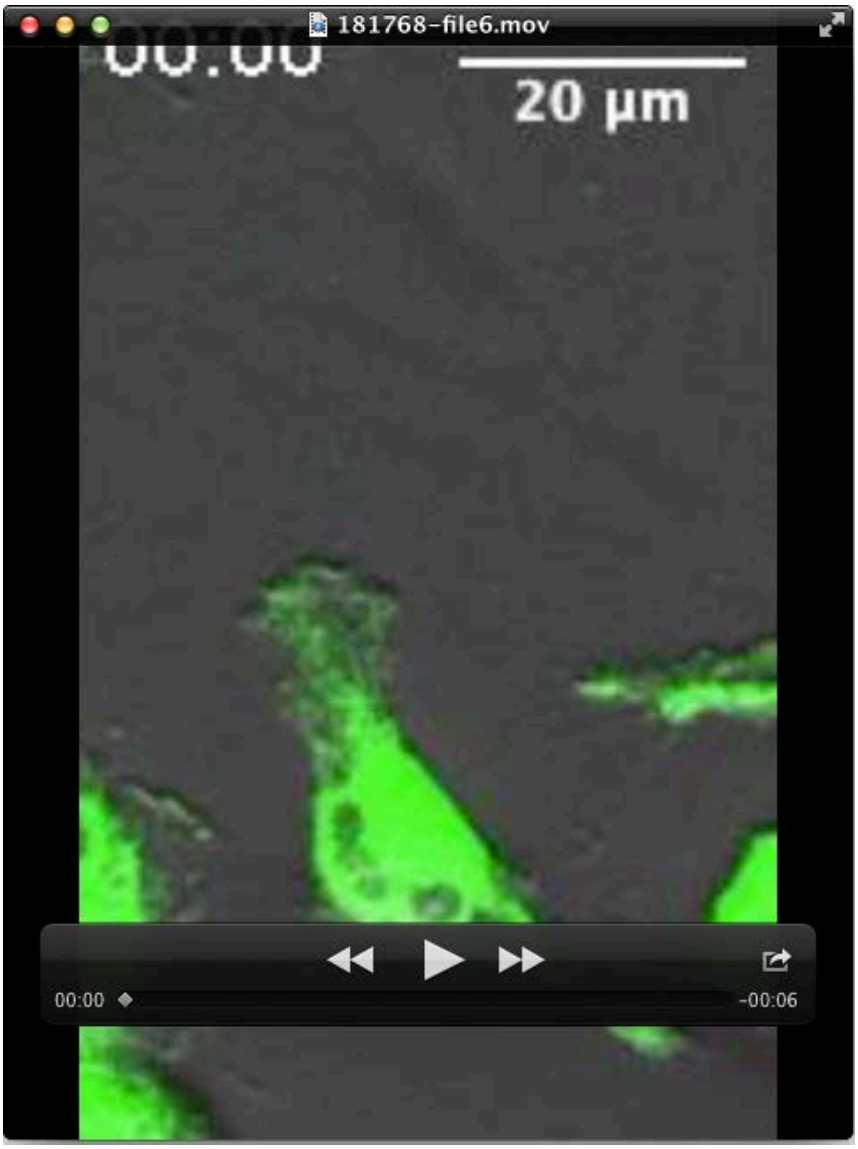

Movie S6| Dynamics of ER in bifurcating protrusion. MDA-MB-231 cells were stained with ER Tracker Blue-White DPX and were allowed to migrate towards 10% FBS in Dunn chamber. Direction of chemoattractant gradient is towards the top.